applied sciences

MDPI

Article

Optimization of Growth Conditions for *Magnetospirillum magnetotacticum* and Green Synthesis of Metallic Nanoparticles

Rebekah Eleasa Sancho [1], Anushka Govindsamy [2] and Karen Pillay [1,*]

[1] School of Life Sciences, University of KwaZulu-Natal, Private Bag X54001, Durban 4001, South Africa
[2] Health Platform, Nanotechnology Innovation Centre, Advanced Materials Division, Mintek, Private Bag X3015, Randburg 2125, South Africa
* Correspondence: muthusamy@ukzn.ac.za; Tel.: +27-31-2607665

Abstract: Nanotechnology is especially useful in biotechnological and biomedical applications as nanomaterials have unique physicochemical properties. Current physical and chemical techniques used for the production of nanoparticles have various disadvantages that has led to the evaluation of biological strategies. This study focused on the use of a bacterial species known as *Magnetospirillum magnetotacticum* for the production of metallic nanoparticles. The cultivation of MTB is known to be tedious and time-consuming using the current standardized magnetic spirillum growth media (MSGM). This study explored the optimization of MSGM for improved growth and nanoparticle yield. It was found that glucose significantly improved and sustained the growth of *M. magnetotacticum* compared to other sole carbon sources having a sustainable OD of ~1.15. However, use of a higher concentration of sodium nitrate (40 mM) as a nitrogen source was able to significantly improve iron-containing nanoparticle yield by 1.6× with a final yield of 22 mg/50 mL when compared to the yield obtained from the MSGM original media. Growth media with a combination of glucose, sodium nitrate, ammonium sulphate and yeast extract showed the highest exponential growth of *Magnetospirillum magnetotacticum* compared to all other MSGM modifications with the highest OD being 1.7. Silver and gold nanoparticles were also successfully produced in addition to iron-containing nanoparticles. Overall, no direct correlation between growth and nanoparticle yield was found.

Keywords: optimization; magnetic spirillum growth media (MSGM); metallic nanoparticle yield; growth conditions

check for updates

Citation: Sancho, R.E.; Govindsamy, A.; Pillay, K. Optimization of Growth Conditions for *Magnetospirillum magnetotacticum* and Green Synthesis of Metallic Nanoparticles. *Appl. Sci.* **2023**, *13*, 8491. https://doi.org/10.3390/app13148491

Academic Editors: Murtaza Hasan and Xugang Shu

Received: 23 May 2023
Revised: 5 July 2023
Accepted: 11 July 2023
Published: 22 July 2023

Copyright: © 2023 by the authors. Licensee MDPI, Basel, Switzerland. This article is an open access article distributed under the terms and conditions of the Creative Commons Attribution (CC BY) license (https://creativecommons.org/licenses/by/4.0/).

1. Introduction

Physical and chemical techniques for the synthesis of nanoparticles involve complex protocols, high temperature requirements and the employment of hazardous compounds such as reducing agents, which not only leads to expensive costs but also the formation of toxic pollutants on the surfaces of the nanoparticles synthesized. The aspects mentioned not only cause uncertainty in the preparation steps but also directly question their applicability in biological systems. On the contrary, the synthesis of nanoparticles via green technology, also known as biological synthesis, makes use of biological organisms that are cost-effective, omits use of toxic chemicals and rather utilizes an eco-friendly approach of synthesis that has gained precedence over conventional physical and chemical techniques.

Nanoparticle synthesis carried out by bacteria has gained interest due to their advantageous properties which include high growth rate, ease of cultivation and ability to grow in unfavourable environmental parameters (e.g., temperature, pH and pressure) [1]. The difference between bacteria and other green synthetic strategies such as plants is that bacteria can be genetically moulded and manipulated with ease for the biomineralization of metal ions. On the contrary, the use of plants for the synthesis of nanoparticles is not feasible as it is difficult to control growth parameters due to climate and environmental factors, and

to regulate plant growth conditions sophisticated facilities, e.g., greenhouses are required which are not cost-effective as they require a lot of equipment and maintenance. Plants also require a long growth period before any part of the plant can be harvested for use whereas bacteria have a much quicker cultivation period and thus are of particular interest.

Magnetotactic bacteria (MTB) can be described as aquatic prokaryotes whose movement is directed by the Earth's externally applied magnetic and geomagnetic fields due to their ability to exhibit magnetotactic behaviour known as 'magnetotaxis'. These bacteria represent a morphologically, phylogenetically and physiologically diverse group of Gram-negative bacteria known to biomineralize unique organelles referred to as 'magnetosomes' [2,3]. Magnetosomes contain nano-sized particles composed of either magnetite (Fe_3O_4) or greigite (Fe_3S_4) depending on the species used, and these iron-containing particles are encased in a lipid bilayer membrane referred to as the magnetosomal membrane [3–5].

MTB-produced nanoparticles have garnered a lot of interest as these nanoparticles have a number of desirable properties that are not often present in physically and chemically synthesized nanoparticles, such as narrow size distribution, uniform morphology, a large single magnetic domain, and high levels of purity and stability [6,7]. MTB-produced nanoparticles also have the added advantage of being easily dispersible and having facile functionalization due to their magnetosomal membrane [8]. The surface properties of magnetosomes allow significant amounts of specific molecules to be anchored on to the membrane which enables easy functionalization for various applications dealing with cell specific targeting [9]. Interestingly, these nanoparticles have been investigated as biotechnological tools in various applications which include but are not limited to drug delivery, cell separation, food safety, magnetic resonance imaging (MRI) contrast agents, antimicrobial agents and antioxidant agents, as well as other applications such as recovery or detection of DNA or antigens, hyperthermia treatment, enzyme immobilization and environmental applications focusing on wastewater treatment [10]. Synthesizing magnetosomes on a large scale for commercial applications is still quite challenging. The necessity for high magnetosome yield at affordable expenditure and energy cost is the main impediment to industrial-scale mass production of magnetosomes.

Although it is relatively straightforward to identify MTB in samples obtained from natural settings, they are known as a fastidious group of prokaryotic organisms that require specific cultivation conditions for growth and isolation [11]. The yield of magnetosomes synthesized by MTB can theoretically be increased by optimizing the culture medium composition and growth conditions [12]. However, there have only been a few studies that have concentrated on this type of optimization. Temperature, dissolved oxygen, pH, and concentrations of various salts and acids have all been studied in relation to growth, but a greater focus on maximization of magnetosome yield is required [13]. The concentration of nutrients, particularly carbon and nitrogen sources, are amongst the most important elements impacting MTB development and, as a result, magnetosome formation [14].

The cultivation of MTB is known to be tedious and time-consuming using the current standardized magnetic spirillum growth media (MSGM). Therefore, this study explored the optimization of MSGM for improved growth and nanoparticle yield in the MTB species, *Magnetospirillum magnetotacticum*.

2. Materials and Methods

2.1. Materials

The microaerophilic, magnetotactic bacterial species *M. magnetotacticum* strain MS-1 used in this study was purchased from Deutsche Sammlung von Mikro-organismen und Zellkulturen (DSMZ, Brunswick, Germany). Isolation of the nanoparticles was carried out using a MACS column and magnetic stand (Miltenyi Biotec, Bergisch Gladbach, Germany). All materials used in this study including the chemicals, solvents and reagents were of molecular biology or tissue culture grade and purchased from Sigma-Aldrich (St. Louis, MO, USA), unless otherwise stated.

2.2. Growth Media Preparation

The medium used for the modifications presented in this study was the revised magnetic spirillum growth medium (MSGM) and was prepared in accordance with the instructions given by the ATCC (ATCC revised medium 1653) shown in Table S1 (Supplementary Material), with the addition of Wolfe's Mineral Solution as well as Wolfe's Vitamin Solution indicated in Table S2 (Supplementary Material). MSGM was prepared following the addition of individual components according to Table S1 and dissolving in water with continuous stirring. Thereafter, the pH was adjusted to 6.8 using sodium hydroxide (NaOH) and the medium was autoclaved at 121 °C for 20 min. The medium was then allowed to cool to room temperature before use and MSGM original (i.e., no modifications) served as the control medium.

2.3. Metal Stock Solutions

The following metals were used: iron (Fe), silver (Ag), gold (Au) and zinc (Zn). A 10 mM stock solution of each metal was made up using each metal salt and sterile distilled water (dH_2O) to a total working volume of 100 mL each. The iron solution used was ferric quinate, where ferric chloride (0.27 g) and quinic acid (0.19 g) were added to a total volume of 100 mL of dH_2O. Since MTB have the natural ability for iron uptake and to biomineralize it into magnetosomes, iron was selected as the primary metal stock solution that served as the control metal for each medium being modified. Thereafter, the following metal salts were used to make up each of the other three metal stock solutions to a total volume of 100 mL each: silver nitrate (0.17 g), gold (III) chloride trihydrate (0.39 g) and zinc chloride (0.14 g). A 2 mL volume of each metal stock solution was added to each medium prior to bacterial growth.

2.4. Bacterial Growth Curves

M. magnetotacticum was grown in media that varied in composition, to evaluate which carbon and nitrogen source resulted in a quicker culturing time, and overall increased cell biomass and nanoparticle yield. Tubes were sealed with parafilm to maintain microaerophilic conditions and incubated at 30 °C for 336 h. This was performed to determine which components were needed to develop an overall optimized medium. Each medium prepared was sterilized using an autoclave for 20 min at 121 °C, then cooled to room temperature before use.

The use of lactate or lactic acid as a carbon source has been widely studied in *M. gryphiswaldense* bioreactor experiments; thus, lactic acid was selected for investigation as a potential carbon source [15]. In addition, glucose and sodium pyruvate were also selected as potential carbon sources. According to a study carried out by Jajan et al., 25 mM was found to be the optimum concentration for sodium pyruvate [16]. Thus, 25 mM was employed for all three sole carbon sources investigated for the amount of carbon present in the growth media to be kept constant upon comparison of the results.

Thereafter, the original nitrogen source present in MSGM, namely sodium nitrate (1.4 mM), was replaced with a different sole nitrogen source. According to comparisons made from different studies, ammonium sulphate, ammonium chloride and sodium nitrate have all been utilized previously [6,17–19]. Thus, these components were investigated for use as potential nitrogen sources at a concentration of 40 mM in our study as per a previous study by Jajan et al. (2019) who used 40 mM sodium nitrate [16]. The concentration was kept constant to ensure that the amount of nitrogen present in these sources remained the same allowing for a fair comparison to be made. In addition, certain medium modifications were supplemented with one of two additives, namely yeast extract or Isogro™ (Sigma-Aldrich, St. Louis, MO, USA).

Bacterial growth curves were conducted for each MSGM medium modification that are depicted in Table S3 (Supplementary Material). The initial optical density (OD) range for each growth curve sample at time point zero was standardized between a range of 0.1 to 0.2 using an ultraviolet–visible (UV-vis) spectrophotometer (Specord® 210 UV/Vis

spectrophotometer, Analytik Jena, Jena, Germany). The wavelength of the absorbance readings taken for each of the medium modifications was 600 nm except in the case of MSGM containing sodium pyruvate and lactic acid, where the wavelength used was 450 nm due to the change in colour of the media to bluish-purple.

The growth curve experimental design was made up of two biological replicates and in each instance three technical replicates per sample were used to ensure reproducibility. The OD readings were taken at time zero (T0) and thereafter every hour for six hours (T0–T6). Subsequent to the 6 h, the OD readings were taken every 24 h for 14 days (336 h) to monitor whether a prolonged incubation time resulted in increased or decreased growth.

2.5. Metallic Nanoparticle Production in M. magnetotacticum

M. magnetotacticum was grown in MSGM original followed by each of the different medium modifications containing the control metal iron for the preparation of nanoparticles. MS-1 bacterial stock (5 mL) was inoculated into an airtight tube containing 45 mL of growth medium of each MSGM medium modification. Tubes were sealed with parafilm to maintain microaerophilic conditions and incubated at 30 °C for 48 h. Thereafter, OD readings were taken, and 50 µL from each of these tubes were kept for TEM and EDX analysis. Three untouched tubes were used for nanoparticle isolation and to obtain the nanoparticle dry yield. Thereafter, *M. magnetotacticum* was grown in MSGM original and two growth media that showed the most favourable nanoparticle production (i.e., MSGM + sodium nitrate (40 mM) and MSGM + sodium nitrate + Isogro™) using each of the other three metals namely silver, zinc and gold following the same growth conditions as mentioned above.

2.6. Metallic Nanoparticle Isolation

2.6.1. Nanoparticle Isolation Using MACS Column

Iron, silver and gold nanoparticles were isolated using a MACS column (Miltenyi Biotec, Bergisch Gladbach, Germany) that consisted of a ferromagnetic bead (spherical) matrix. When the column was attached to the strong magnetic stand, an intense magnetic field surrounded the column, which resulted in a high magnetic field gradient that had the ability to separate the magnetic samples. With the nanoparticles being smaller in size compared to the beads within the column, the nanoparticles were able to freely pass though the column. This provided an efficient way to elute the particles remaining in the column when the column was removed from the magnetic stand.

The isolation process involved centrifugation of the 50 mL culture tubes at 4000 rpm for 20 min at 4 °C, to first pellet the cells. Thereafter, the supernatant was removed, and the pellet was re-suspended in 10 mL of 20 mM HEPES- 4 mM EDTA (pH 7.4), followed by brief vortexing to disrupt the pellet. The suspension was then sonicated for 10 min to break open the cells. Thereafter, the suspension was centrifuged at 4000 rpm for 15 min at 4 °C to pellet the cell debris, as well as the unbroken cells from the nanoparticles that remained in the supernatant. The supernatant was then transferred to a new tube and passed through the MACS magnetic separation column attached to the magnetic stand. The column was then rinsed with 20 mL 10 mM HEPES-200 mM NaCl and washed with 20 mL 10 mM HEPES. Thereafter, the column was removed from the magnetic stand and placed over a new, pre-weighed tube, where the purified nanoparticles were eluted from the column using 5 mL of 0.01 M HEPES buffer to concentrate the nanoparticles. The eluted nanoparticle solution was then dried in an oven set at 80 °C. The dry weight of the nanoparticles was then ascertained.

2.6.2. Nanoparticle Isolation Using Ultracentrifugation

Zinc nanoparticles were isolated primarily via ultracentrifugation as zinc is known to be diamagnetic in nature [20]. Thus, nanoparticle isolation via the MACS column would not be an appropriate choice for zinc as the zinc nanoparticles would repel the magnetic field resulting in unsuccessful retention of the nanoparticles in the MACS column.

The preparation steps before ultracentrifugation were based on the initial steps outlined in Section 2.6.1 above with slight modifications that involved centrifugation of the 50 mL culture tubes at 4000 rpm for 30 min at 4 °C, to first pellet the cells. Thereafter, the supernatant was removed and the pellet was re-suspended in 10 mL of 20 mM HEPES-4 mM EDTA (pH 7.4), followed by brief vortexing to disrupt the pellet. The suspension was then sonicated for 30 min to break open the cells. Thereafter, the suspension was centrifuged at 4000 rpm for 10 min at 4 °C to pellet the cell debris, as well as the unbroken cells from the nanoparticles which remained in the supernatant. The supernatant was then transferred to an ultracentrifuge tube and centrifuged at 13,000 rpm for 30 min. Thereafter, the sample was decanted and the pellet was resuspended in 500 µL of sterile dH_2O. The pellet was then sonicated for 5 min, vortexed for ~5 min and transferred to pre-weighed Axygen® MAXYMum recovery® microtubes (Corning Incorporated, Reynosa, Mexico). Lastly, the samples were dried in an oven set at 80 °C for approximately 2–3 days. The dry weight of the nanoparticles was then ascertained.

2.7. Characterization of the Nanoparticles

Characterization techniques were adapted from Moodley et al. (2018) [21,22]. Reconstituted metallic nanoparticle samples and whole bacterial cells present in growth media were used in transmission electron microscopy (TEM) and elemental dispersive X-ray analysis whereas only reconstituted nanoparticle samples were used for dynamic light scattering (DLS) analysis.

2.7.1. Transmission Electron Microscopy (TEM) and Energy Dispersive X-ray Analysis (EDX)

Characterization of the samples was performed via high-resolution transmission electron microscopy (HRTEM) using a JEOL JEM-2100 electron microscope (Tokyo, Japan) operating at 200 kV and 0.23 nm resolution. The electron source used was a lanthanum hexaboride (LaB6) filament. The sizes of the nanoparticles and data analysis of their sizes were achieved using Image J software v1.53t (National Institutes of Health, Bethesda, MD, USA) [23]. The samples were also analysed via EDX (X-Max 80 mm silicon drift detector (SDD), Oxford Instruments, High Wycombe Buckinghamshire, UK) using INCA v 4.15 software (Oxford Instruments, High Wycombe Buckinghamshire, UK) to determine their elemental compositions in order to verify whether the metals under investigation were present.

Sample preparation was conducted as follows; a 5 µL drop of each sample was pipetted onto a carbon coated copper TEM grid and allowed to stand at room temperature for 2 min. The excess fluid was removed using filter paper and thereafter a 5 µL drop of distilled water was added and once again removed using filter paper to wash off any excess media. The grids were then air dried at room temperature for at least 2 h before being analysed.

2.7.2. Dynamic Light Scattering (DLS)

The reconstituted nanoparticle samples were analysed via DLS using a Malvern Zetasizer Nano ZS instrument operating on software version 8.02 (Worcestershire, UK), to determine the size and zeta potential of the nanoparticles synthesized. Sample preparation involved dilution of the nanoparticle samples using sterile dH_2O. DTS0012 polystyrene cuvettes were used for sizing whereas DTS1070 zeta cells were used for determination of the zeta potential.

2.8. Statistical Analysis

All data were statistically analysed using GraphPad InStat version 3.10 for Windows (GraphPad Software, San Diego, CA, USA). Growth curve data were subjected to an analysis of variance (ANOVA). Differences were considered significant when $p < 0.05$. To compare the trends of the different growth curves, Pearson's correlation coefficient (r) was used. Correlation coefficients ranging from 0.7 to 1.0 indicate a high level of corre-

lation, 0.4–0.69 indicates moderate correlation and 0–0.39 indicates low correlation [24]. To attain the level of polydispersity, the polydispersity index (PDI) values were used. PDI values > 0.7 indicate very polydisperse samples, 0.08–0.7 indicates mid-range polydispersity, 0.05–0.08 indicates nearly monodisperse samples and 0–0.05 indicates monodisperse samples. Detailed results from statistical analysis are presented in the Supplementary Material in Tables S5 and S6.

3. Results and Discussion

Carbon and nitrogen sources serve as essential nutritional requirements for bacterial cell growth. The concentration of carbon and nitrogen sources present in growth media are amongst the most important elements impacting MTB development and, as a result, magnetosome formation [14]. The present study investigated the use of different carbon and nitrogen sources in order to find suitable sole carbon and nitrogen sources that could both optimize growth and improve magnetosome production whilst being cost efficient. When analysing the effect of the carbon source modification on growth of *M. magnetotacticum*, it was found that comparatively growth was slow in the unmodified MSGM (MSGM) with no distinct peak and no distinct phases of growth (Figures 1 and 2). A graph with all growth curves on a single set of axes is available in the Supplementary Material as Figure S1. There was a gradual increase in OD as time progressed; however, the growth did not exceed an OD of 0.287 even after 336 h of incubation.

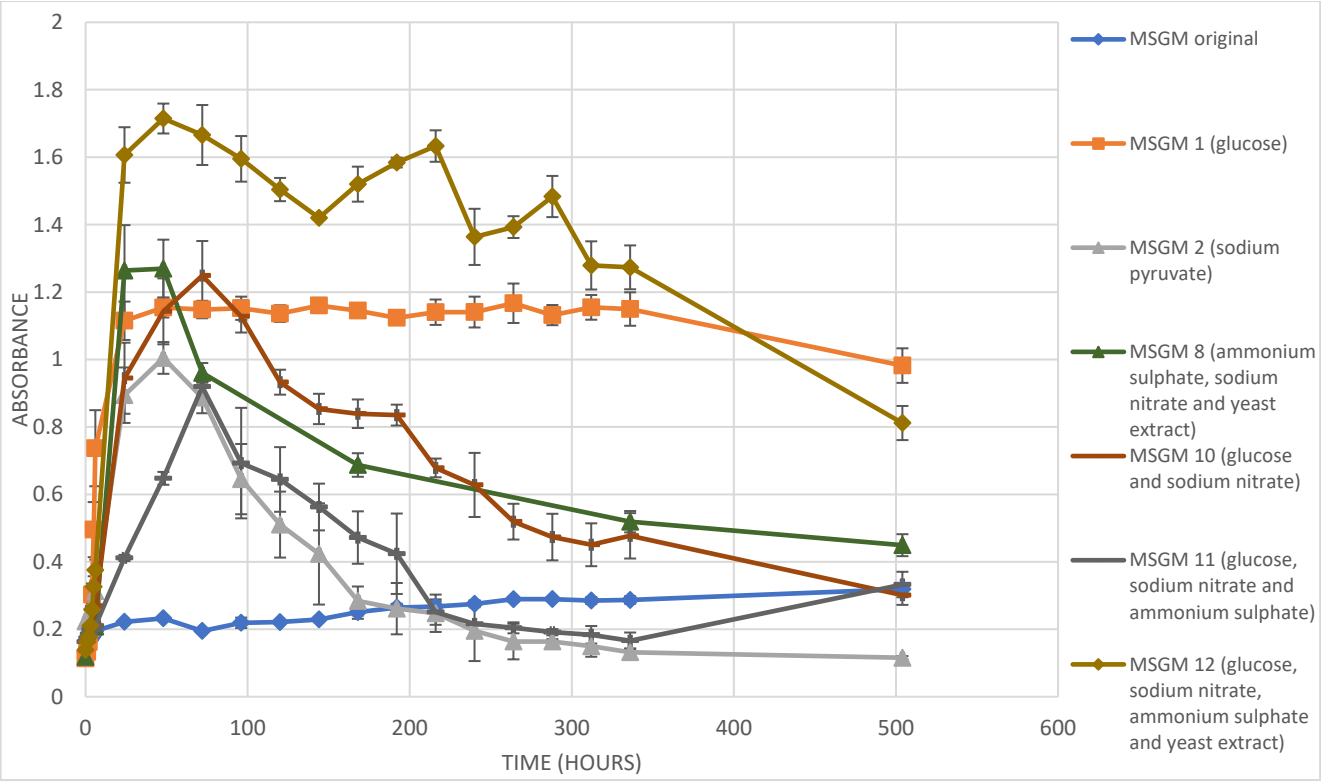


Figure 1. Growth curves of *M. magnetotacticum* in MSGM original and medium modifications MSGM 1, 2, 8, 10, 11 and 12 at 30 °C with iron as the metal source. OD readings were taken at a wavelength of 600 nm for MSGM, MSGM 1, MSGM 8 and MSGM 10–12, and at 450 nm for MSGM 2.

Improved growth of *M. magnetotacticum* was observed in MSGM media containing sodium pyruvate (MSGM 2) compared to MSGM original. During the exponential phase between 0 and 48 h, a maximum OD of 1.005 was observed. This finding was supported by Jajan et al. (2019) who used *M. gryphiswaldense* strain MSR-1 and four different carbon sources (sodium pyruvate, sodium L-lactate, sodium succinate and sodium acetate), and

reported that sodium pyruvate and sodium L-lactate significantly increased the cell growth, cellular magnetotactic response (Cmag), rate of Fe uptake and magnetosome production when compared to sodium succinate and sodium acetate as the carbon source [16]. Their results also showed that sodium pyruvate (25 mM) was much more effective at increasing magnetosome production. Results from the present study thus indicate that sodium pyruvate contributes to rapidly dividing bacterial cells; however, a rapid decline could be noted after the peak had been obtained indicating that this carbon source was depleted quite quickly. It is thus possible that limited vital nutrients could have led to death of the cells.

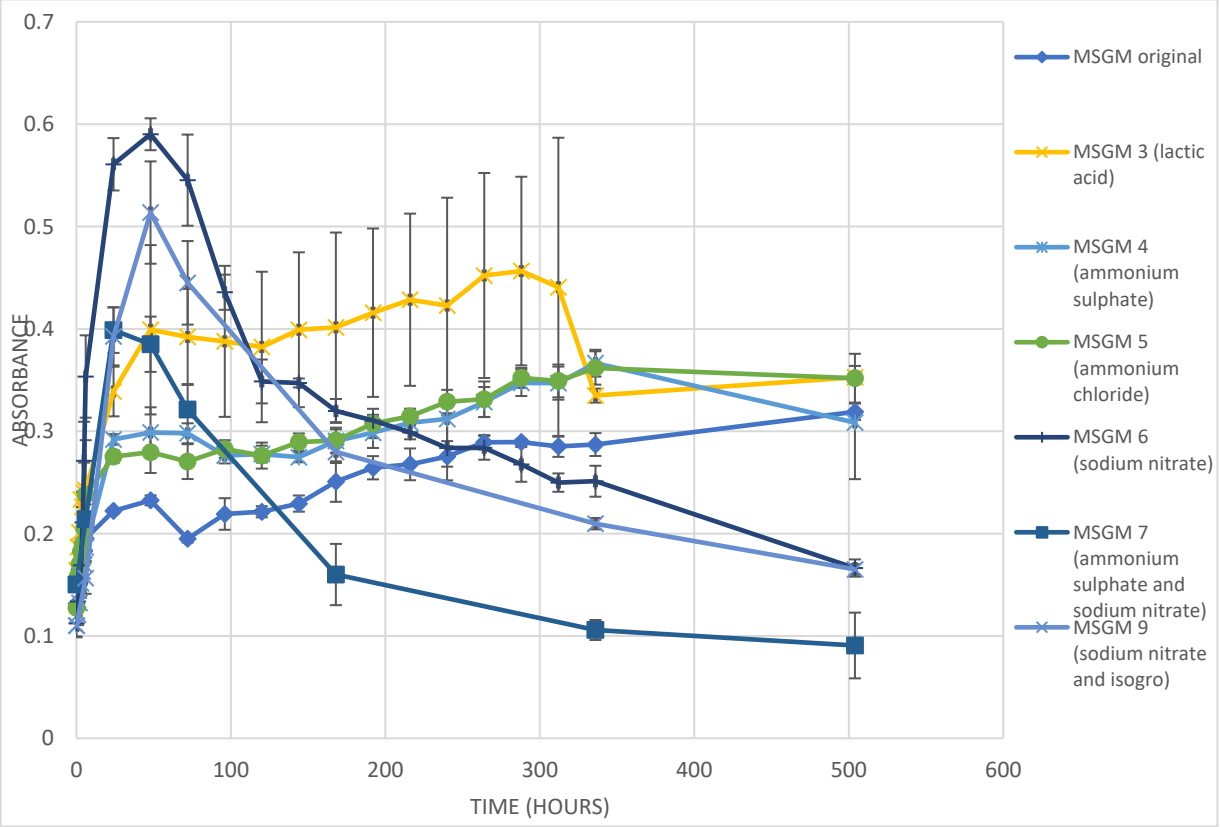


Figure 2. Growth curves of *M. magnetotacticum* in MSGM original and medium modifications MSGM 3–7 and MSGM 9 at 30 °C with iron as the metal source. OD readings were taken at a wavelength of 600 nm for MSGM, MSGM 4–7 and MSGM 9, and at 450 nm for MSGM 3.

Growth of *M. magnetotacticum* in MSGM 2 was also greater than MSGM containing lactic acid (MSGM 3) which produced a maximum OD of 0.46 after 288 h of incubation. In addition, the results showed that the lactic acid modification (MSGM 3), compared to the original MSGM, had an r value of 0.83. The high level of correlation could be attributed to both of these media having no distinct phases of growth.

The third sole carbon source used in this study was glucose as it is a well-known carbon source that is preferred for bacterial growth (e.g., *E. coli*), and is a known source of energy for all organisms as it is essential to fuel both aerobic and anaerobic cellular respiration [25,26]. Glucose is also a cheaper alternative to the three combined carbon sources used in MSGM (i.e., ascorbic acid, succinic acid and tartaric acid) and is commonly used in bacterial growth media. When glucose was utilized as the sole carbon source (MSGM 1), the highest and most sustainable growth of *M. magnetotacticum* was observed compared to using growth media MSGM 2, MSGM 3 and even MSGM the original medium which had three carbon sources. When *M. magnetotacticum* was grown in MSGM 1, a peak OD of 1.15 was observed after only 48 h and this peak was sustained for 336 h.

The nitrogen source modifications were thereafter performed. Jajan et al. (2019) investigated three nitrogen sources which included sodium nitrate, ammonium chloride and ammonium sulphate. It was found that sodium nitrate increased the cellular magnetotactic response (Cmag), rate of Fe uptake and magnetosome production significantly when compared to the other two nitrogen sources. The concentration used for sodium nitrate in the optimized culture medium which was found to increase cell growth and magnetosome production was 40 mM [16,19,27]. In addition, nitrates such as sodium nitrate are a commonly used nitrogen source for *Magnetospirillum* bacteria [3]. The nitrogen source present in MSGM original, 1.4 mM sodium nitrate, was modified and increased to 40 mM and the type of nitrogen source was also investigated in this study, by using ammonium sulphate (40 mM) and ammonium chloride (40 mM). The modifications using ammonium sulphate (40 mM) (MSGM 4) and ammonium chloride (40 mM) (MSGM 5) showed a very similar growth trend to that of the MSGM original (containing 1.4 mM sodium nitrate), with r values of 0.91 and 0.97 (Table S4 in Supplementary Material), respectively, indicating a very high positive correlation to MSGM original. This indicated that there were no distinct phases of growth when either ammonium sulphate or ammonium chloride were used, and thus these two nitrogen sources even at a high concentration of 40 mM did not improve bacterial growth. However, when the concentration of sodium nitrate was increased from 1.4 mM (MSGM original) to 40 mM (MSGM 6) there was a significant increase in bacterial growth, with the highest OD being 0.590 after 48 h of incubation. An r value of 0.15 was obtained when compared to MSGM original, which indicates a negligible correlation to that of MSGM original possibly due to the distinct exponential phase of growth between 0 and 48 h of incubation.

The present study thus supports the findings of Jajan et al. (2019) [16]. However, according to a study by Liu et al. (2010), ammonium chloride was identified as a better nitrogen source for growth and the discrepancy in findings may be attributed to the nature of the experiment [27]. The experiment by Liu et al. (2010) took place on a larger scale with the concentration of nitrogen being auto-controlled at a constant level via the use of pH-stat feeding thus enabling ease of manipulation and elimination of the possibility of nutrient exhaustion during the culture process which would otherwise occur in a laboratory-based experiment such as in the present study [27].

The use of two nitrogen sources namely ammonium sulphate (40 mM) and sodium nitrate (40 mM) used in combination (MSGM 7) was also investigated. However, *M. magnetotacticum* still showed better growth when sodium nitrate (40 mM) was the sole nitrogen source (MSGM 6) as per Figure 2. The peak OD of *M. magnetotacticum* grown in MSGM 7 was below that of the MSGM modification which used sodium nitrate (40 mM) as the sole nitrogen source (MSGM 6). Due to an increase in nitrogen availability in MSGM 7, it could be argued that more magnetosomes were produced and as a result nutrient depletion occurred faster, resulting in slower growth of *M. magnetotacticum* in MSGM 7 than in MSGM 6 media. However, slower growth due to the potential toxic effect of the magnetosomes themselves and/or their excretion can be ruled out as growth curves were also compared to nanoparticle yield as shown in Section 3.2 below; thus, nutrient depletion is the most probable factor.

Yeast extract was then used as an additional nutrient source (medium modification MSGM 8) and notably the second highest growth was obtained (OD of 1.27), establishing that use of an additive benefits *M. magnetotacticum* growth. Since the additive yeast extract improved growth, we set out to establish whether another additive Isogro™ could also perform similarly. Isogro™ is composed of an algal lysate that contains metabolic precursors permitting the bacteria to initiate growth more rapidly, thus eliminating the need for de novo production of the various components of the metabolic pathways. Isogro™ was then added to MSGM 6 since MSGM 6 resulted in the best bacterial growth amongst all nitrogen sources tested. This modification resulted in MSGM 9; however, *M. magnetotacticum* growth did not improve when compared to MSGM 6 and in fact remained similar ($p > 0.05$),

possibly due to it not containing the specific nutrient requirements needed for improved growth for this particular bacterial species.

Since the highest growth of *M. magnetotacticum* was obtained in MSGM media containing glucose and sodium nitrate as the sole carbon and nitrogen sources, respectively, these nutrient sources were combined to create the MSGM modification MSGM 10. *M. magnetotacticum* grown in MSGM 10 reached an OD of 1.25 after 72 h of incubation. However, a rapid decline could be noted once the highest growth had been obtained and thus there was no prolonged sustainable growth as that seen when using glucose alone. Upon addition of ammonium sulphate to the MSGM modification containing glucose and sodium nitrate to produce MSGM 11, it could be noted that the presence of two nitrogen sources resulted in a lower growth with an OD of 0.92 after 72 h of incubation and also resulted in a more pronounced decline after the exponential phase was concluded which was below that of MSGM 10 (modification using glucose and sodium nitrate in combination).

Thereafter, glucose, ammonium sulphate, sodium nitrate and yeast extract were combined resulting in MSGM 12. This modification was performed to establish whether the addition of two nitrogen sources having a higher growth rate than MSGM original, together with the best carbon source and an additive, were able to improve *M. magnetotacticum* growth. When yeast extract was added, an almost two-fold improvement in *M. magnetotacticum* growth (OD 1.71) was observed when compared to MSGM 11. Comparatively, the highest growth of *M. magnetotacticum* was obtained using MSGM 12 consisting of glucose as the sole carbon source, two nitrogen sources namely sodium nitrate and ammonium sulphate, and the additive yeast extract.

3.1. Metallic Nanoparticle Synthesis by M. magnetotacticum Using Either Fe, Ag, Au or Zn

Based on the growth curves obtained in Figures 1 and 2, a peak in *M. magnetotacticum* growth was observed after 48 h of incubation in MSGM and MSGM medium modifications. Therefore, 48 h was selected as the point of isolation of nanoparticles from the various modifications. Dry weight yields of iron-containing nanoparticles produced by *M. magnetotacticum* are presented in Table 1 below.

Table 1. Dry weight yields of iron-containing nanoparticles produced by *M. magnetotacticum* and isolated after 48 h of incubation at 30 °C in different media.

Medium Modifications	Nanoparticle Yield (mg/50 mL)
MSGM original	14
MSGM 1 (glucose)	14
MSGM 2 (sodium pyruvate)	15
MSGM 3 (lactic acid)	15
MSGM 4 (ammonium sulphate)	20
MSGM 5 (ammonium chloride)	15
MSGM 6 (sodium nitrate)	22
MSGM 7 (ammonium sulphate and sodium nitrate)	18
MSGM 8 (ammonium sulphate, sodium nitrate and yeast extract)	21
MSGM 9 (sodium nitrate and Isogro™)	17
MSGM 10 (glucose and sodium nitrate)	16
MSGM 11 (glucose, sodium nitrate and ammonium sulphate)	20
MSGM 12 (glucose, sodium nitrate, ammonium sulphate and yeast extract)	20

M. magnetotacticum synthesis of Fe nanoparticles in MSGM original resulted in a yield of 14 mg/50 mL which was found to be similar ($p > 0.05$) to yields from all three sole carbon source modifications, i.e., MSGM 1, MSGM 2 and MSGM 3 having yields of 14 mg/50 mL, 15 mg/50 mL and 15 mg/50 mL, respectively. This indicated that the original carbon sources present in MSGM (i.e., ascorbic acid, succinic acid and tartaric acid) could be replaced by any one of the three sole carbon sources without significantly impacting *M. magnetotacticum* nanoparticle yield.

However, when *M. magnetotacticum* was grown in a modified MSGM medium with a higher concentration of sodium nitrate (40 mM) (MSGM 6), there was an extremely significant difference observed ($p < 0.001$) with a yield of 22 mg/50 mL being obtained. This indicated that, by increasing the concentration of sodium nitrate, the nanoparticle yield improves. Thus, the role of nitrogen is very important to form proteins for the assembly of magnetosomes, and to transport and incorporate iron in MTB. These findings can be supported by Jajan et al. (2019) who showed that the use of sodium nitrate in particular led to a higher production of magnetosomes as observed in our study, possibly due to nitrate being a strong oxygen acceptor having redox potential [16]. In addition, a study by Bazylinski and Blakemore (1983) found that *M. magnetotacticum* was able to reduce nitrate mainly to N_2O or N_2 while producing magnetosomes, indicating the existence of a functioning denitrification mechanism in MTB suggesting that it may be involved in the synthesis of magnetite and thus magnetosome production as mentioned by Yamazaki et al. (1995) and Taoka et al. (2003) [28–30].

Interestingly, by replacing the original 1.4 mM sodium nitrate in *M. magnetotacticum's* growth medium (MSGM) with ammonium sulphate (40 mM) (MSGM 4), it resulted in an extremely significantly different ($p < 0.001$) nanoparticle yield of 20 mg/50 mL. However, no significant difference was observed ($p > 0.05$) in nanoparticle production when *M. magnetotacticum* was grown in either MSGM 4 (40 mM ammonium sulphate) or MSGM 6 (40 mM sodium nitrate) implying that they both significantly increase nanoparticle production and thus the use of either nitrogen source is optimal for nanoparticle production. Similarly, 1.4 mM sodium nitrate was replaced with ammonium chloride (40 mM), but there was no significant difference observed between nanoparticle yield from MSGM original and nanoparticle yield from MSGM 5 (ammonium chloride). Thus, replacing the original nitrogen source of sodium nitrate (1.4 mM) with ammonium chloride (40 mM) did not improve nanoparticle yield.

When the three original carbon sources were combined with two nitrogen sources namely ammonium sulphate (40 mM) and sodium nitrate (40 mM) resulting in MSGM 7, a yield of 18 mg/50 mL was obtained that was significantly different ($p < 0.05$) from MSGM original indicating that there was an improvement in nanoparticle yield when compared to MSGM original. Comparison of MSGM 7 to the medium with the highest yield, namely MSGM 6, indicated that there was no significant difference ($p > 0.05$), thus increasing the amount of nitrogen present via the use of two nitrogen sources instead of one did not give a further improvement in nanoparticle yield as the maximal nanoparticle producing capacity could have already been achieved. Upon addition of yeast extract, resulting in a medium modification referred to as MSGM 8, there was an extremely significant difference found when compared to MSGM original ($p < 0.001$). However, when MSGM 8 was compared to MSGM 6 and MSGM 7, there was no significant difference observed ($p > 0.05$) leading one to believe that the use of yeast extract did not make a difference in terms of nanoparticle production as there was already an abundance of nutrients present thus accounting for the maximal nanoparticle producing capacity by the bacterial cells.

The addition of Isogro™ to the modification which had the highest yield (MSGM 6) resulted in a medium modification referred to as MSGM 9. This modification was carried out to establish whether this additive would result in a higher nanoparticle yield. The yield obtained for MSGM 9 (sodium nitrate and Isogro™) was 17 mg/50 mL, which was found to not significantly differ when compared to MSGM original ($p > 0.05$). This indicates that Isogro™ was in fact inhibiting nanoparticle production. The addition of Isogro™ may have

created the optimum growth conditions and while this is good for magnetotactic bacterial growth it may have resulted in feedback inhibition of magnetosome production. As mentioned earlier, MTB use the magnetosomes for geomagnetic navigation in their aquatic habitat, i.e., magnetotaxis. It has been proposed that, in natural environments, magnetotaxis may enable the cells to locate and maintain an optimal position in the water column or in sediments, and that this aligns with their main metabolic needs [31]. The magnetic assisted taxis could help MTB in their navigation toward optimum growth conditions [7]; hence, growing MTB under optimum conditions may in fact inhibit magnetosome production.

When medium modification MSGM 10 (glucose and sodium nitrate) was used, the yield obtained was 16 mg/50 mL. Although the sole carbon source and nitrogen source with the highest growth (i.e., glucose (25 mM) and sodium nitrate (40 mM)) were utilized, it was found that the use of both of these nutrient sources did not significantly improve nanoparticle yield when compared to MSGM original ($p > 0.05$). This could be attributable to adequate nutrients being available and thus there is no need for the bacteria to produce magnetosomes in order to facilitate magnetotaxis to a different region [32].

MSGM 11 (glucose, sodium nitrate and ammonium sulphate) and MSGM 12 (glucose, sodium nitrate, ammonium sulphate and yeast extract) produced the same yield (20 mg/50 mL) and were both found to be extremely significantly different when compared to MSGM original ($p < 0.001$). Thus, the use of glucose (25 mM) and two nitrogen sources such as sodium nitrate (40 mM) and ammonium sulphate (40 mM) had allowed *M. magnetotacticum* to reach its full nanoparticle producing potential and the addition of yeast extract to MSGM 12 did not have an additional effect. Interestingly, the additional nitrogen source thus appears to play an important role in magnetosome production. These findings also indicate that a fine balance between carbon and nitrogen sources is required in order to ensure optimal magnetosome production.

Overall, it could be noted that the highest nanoparticle yield was obtained for MGSM 6 (sodium nitrate) having a yield of 22 mg/50 mL; however, when compared to MSGM 4, 8, 11 and 12 with yields of 20 mg/50 mL, 22 mg/50 mL, 21 mg/50 mL, 20 mg/50 mL and 20 mg/50 mL, respectively, it could be noted that there was no statistically significant difference ($p > 0.05$) observed indicating that any of these modifications could be used for optimal nanoparticle production having yields that are significantly different ($p < 0.01$) when compared to MSGM original. In addition, it could be seen that increasing the source of nitrogen beyond a certain point does not increase nanoparticle yield unless there is a component added to the medium that contributes to adequate nutrient supply to the bacteria which could result in inhibition of magnetosome formation since the inherent use of magnetosomes, as described by Müller et al. (2020), is to facilitate transport of the bacterial cells from an area of low nutrient availability to one that has a better amount of nutrients [32].

Since MSGM 6 (40 mM sodium nitrate) had quantitatively shown the highest dry weight of iron-containing nanoparticles, this MSGM modification was then chosen for further analysis. Nanoparticle isolation at all three phases of bacterial growth was carried out using MSGM 6, to ascertain whether the exponential phase (48 h) did indeed result in the highest yield of nanoparticles. According to Table 2 below, the lag phase (24 h) had the lowest yield (16 mg/50 mL) suggesting that the bacterial cells were getting accustomed to their environment in preparation for cell division (i.e., exponential phase) [33]. The exponential phase (48 h) had a yield of 22 mg/50 mL which was the highest yield obtained when compared to the other phases of growth. This can be attributed to the bacteria being the most metabolically active at this phase of growth. The last phase (stationary/death phase) resulted in a yield of 18 mg/50 mL which was indicative of the bacterial cells reaching a plateau in growth.

It could then be confirmed that the exponential phase did result in the highest yield ($p < 0.001$) and was therefore the most effective for isolation of nanoparticles. Furthermore, a study by Marcano et al. (2017) found that when bacteria start synthesizing magnetosomes at the exponential phase of growth they are magnetically closer to stoichiometric magnetite

rather than when they are synthesized at the stationary phase [34]. This further suggests that the synthesis of magnetosomes after 48 h of incubation is more beneficial when compared to the other phases of growth which could also enhance the properties of the nanoparticles produced for potential downstream applicability.

Table 2. Dry weight yield (mg/50 mL) of iron-containing nanoparticles produced by *M. magnetotacticum* and isolated at different phases of bacterial growth after incubation in MSGM 6 at 30 °C.

Bacterial Growth Phase	Time Point (Hours)	Nanoparticle Yield (mg/50 mL)
Lag phase	24	16
Exponential phase	48	22
Stationary/death phase	72	18

According to a study conducted by Heyen and Schuler (2003), a maximum yield of 0.0063 mg/mL was achieved for *M. magnetotacticum* using a medium that varied the iron, nitrogen and carbon source concentrations, containing 27 mM lactate, 4 mM sodium nitrate and 100 µM ferric citrate [6]. It could thus be noted that the medium modification with the highest yield of 0.44 mg/mL obtained in our study (MSGM 6) showed a significant increase in nanoparticle yield as opposed to the study conducted by Heyen and Schuler (2003) [6]. The difference in yield could be attributed to the different iron and carbon sources as well as the lower concentration of sodium nitrate [6]. Another study conducted by Sun et al. (2008) made use of 60 µM ferric citrate, 11.25 mM ammonium chloride and 15 mM of sodium lactate as the iron, nitrogen and carbon sources, respectively [35]. A maximum of 0.0417 mg/mL of iron-containing magnetosomes was achieved after 60 h of incubation using *M. gryphiswaldense*. When comparing our media having the highest yield to their yield, it could be noted that our medium (MSGM 6) had an approximate 11-fold increase in yield which was significantly higher. In addition, another study by Liu et al. (2008) reported the use of ferric citrate, ammonium chloride and sodium lactate in their culture media as iron, nitrogen and carbon sources, respectively, using a chemostat culture technique [36]. A yield of approximately 0.0436 mg/mL was achieved which is ten times less than the yield obtained in the current study using MSGM 6. Interestingly, all studies mentioned above made use of ferric citrate as the iron source when compared to our study that used ferric quinate; thus, the difference in iron sources may have been a contributing factor, i.e., had an effect on the biomineralization process itself, accounting for the significant differences in yield. In addition, it is also quite evident that an optimal nitrogen source is in the form of sodium nitrate at a high concentration of 40 mM.

MSGM original, MSGM 6 and MSGM 9 were then evaluated to determine whether *M. magnetotacticum* was able to use metals such as silver, gold and zinc to synthesize metallic nanoparticles, apart from the inherently biomineralized iron nanoparticles. These metals were selected for this study as they were identified as the most commonly used for downstream application such as antibacterial agents, antioxidant agents, drug delivery and biosensing [21,22,37–44]. According to Table 3 below, *M. magnetotacticum* was unable to synthesize silver nanoparticles when using MSGM original and MSGM 6 (sodium nitrate) respectively as no nanoparticles were visible during TEM analysis and evaluation of elemental composition using EDX did not indicate the presence of silver. However, when Isogro™ was added to the medium resulting in MSGM 9 (sodium nitrate and Isogro™), silver nanoparticles were successfully produced. This suggests that the additive Isogro™ present in MSGM 9 was indeed beneficial for silver nanoparticle production as it allowed for the successful uptake of the metal silver and its subsequent biomineralization into silver-containing nanoparticles as verified by TEM and EDX analysis. All three media evaluated (i.e., MSGM original, MSGM 6 and MSGM 9) were able to be used to successfully synthesize gold nanoparticles as verified by TEM and EDX analysis. Interestingly, MSGM 9

produced an excellent amount of gold nanoparticles when compared to the other medium modifications used. However, in this study using all three media (i.e., MSGM original, MSGM 6 and MSGM 9), zinc nanoparticles could not be synthesized, suggesting that the nature of this bacteria possibly does not favour the production of zinc nanoparticles which can be supported by the fact that no other studies to date have been able to synthesize zinc nanoparticles using *M. magnetotacticum*.

Table 3. Dry weight yield (mg/50 mL) of metallic (Fe, Ag, Au) nanoparticles produced by *M. magnetotacticum* after 48 h of incubation at 30 °C in either MSGM original, MSGM 6 or MSGM 9.

Metallic Nanoparticle	Medium Modification	Nanoparticle Yield (mg/50 mL)
Iron (Fe)	MSGM original	16
	MSGM 6 (sodium nitrate)	22
	MSGM 9 (sodium nitrate and Isogro™)	17
Silver (Ag)	MSGM original	-
	MSGM 6 (sodium nitrate)	-
	MSGM 9 (sodium nitrate and Isogro™)	15
Gold (Au)	MSGM original	17
	MSGM 6 (sodium nitrate)	22
	MSGM 9 (sodium nitrate and Isogro™)	33

Overall, when comparing the bacterial growth to the nanoparticle yields obtained, it could be seen that improved bacterial growth does not necessarily mean an improvement in nanoparticle yield which was evident in MSGM 1, 2 and 10 where improved growth was seen having OD values of 1.14, 1.00 and 1.14 after 48 h of incubation, respectively. However, the nanoparticle yields obtained for these MSGM modifications were found to not statistically significantly differ ($p > 0.05$) from that of MSGM original thereby indicating no improvement in nanoparticle yield. Therefore, according to these results there was no correlation between growth and nanoparticle production in the present study which is in line with the findings of Kresnowati and Wijaya (2016) [45].

3.2. Characterization of Metallic Nanoparticles Synthesized by M. magnetotacticum Using Either Fe, Ag or Au

3.2.1. TEM and EDX Analysis

TEM was used to characterize the morphology of nanoparticles in terms of their shape and size. TEM and EDX analyses were performed for all MSGM modifications (MSGM original and MSGM 1–12) supplemented with iron. The results obtained for MSGM original (Figure 3) indicated that the iron nanoparticles were spherical in shape and well dispersed having narrow size distribution with a size range of 6–7 nm. MSGM 1 which used glucose as a sole carbon source resulted in a cluster of cuboidal-shaped nanoparticles that are characteristic of the *Magnetospirillum* species (Figure S1 in Supplementary Material). However, these nanoparticles were unable to be sized due to aggregation. The nanoparticles synthesized using MSGM 2 (sodium pyruvate) were spherical in shape and larger in size with size ranges of 13–81 nm although most regions were highly aggregated (Figure S3 in Supplementary Material). The use of lactic acid as the sole carbon source (MSGM 3) did not produce well defined nanoparticles but rather a large cluster of undefined particles (Figure S4 in Supplementary Material), and thus could not be sized.

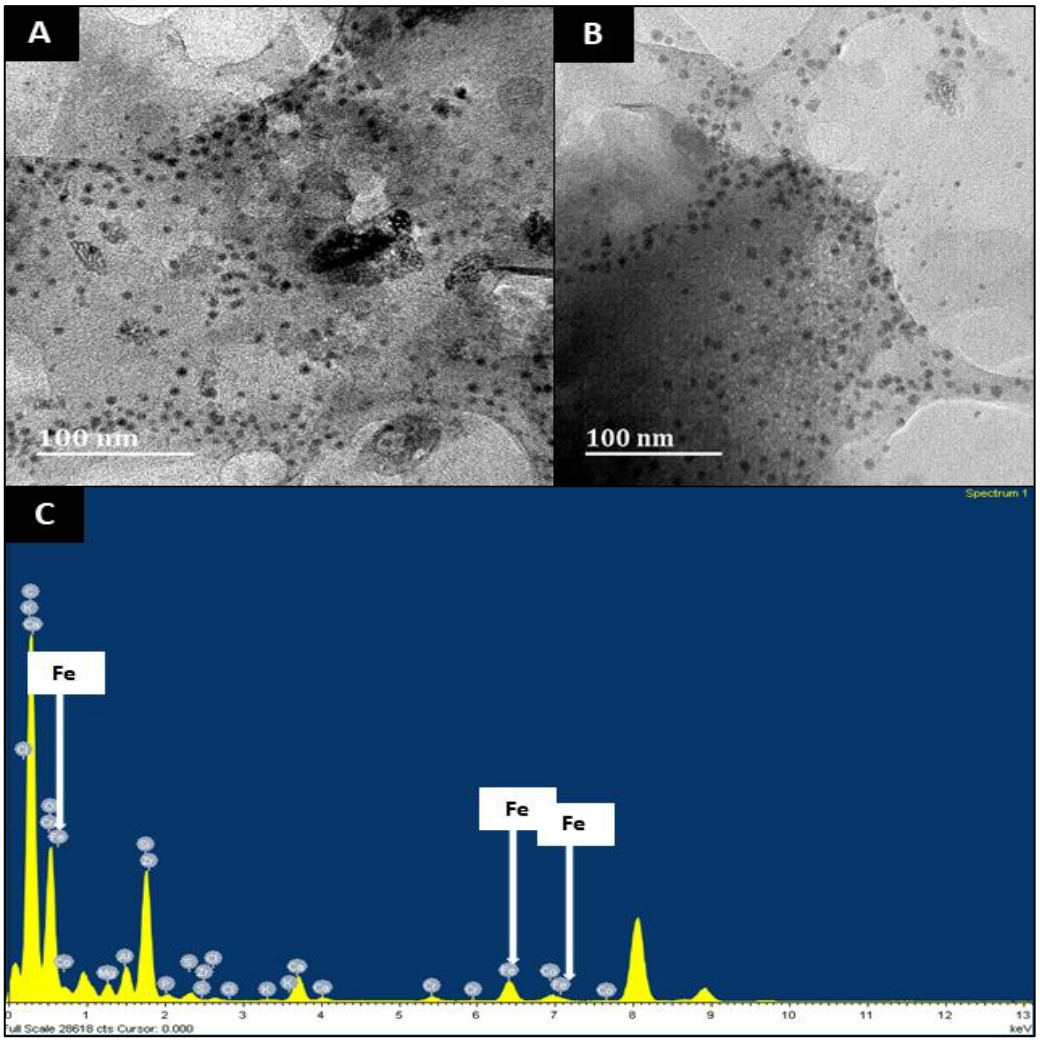


Figure 3. (**A**,**B**) TEM micrographs showing iron-containing magnetosomes formed by *M. magneto-tacticum* after incubation at 30° for 48 h in MSGM original containing iron (10 mM). Size range of nanoparticles is 6–7 nm. (**C**) EDX profile of the observed nanoparticles presented in (**A**). Iron peaks are present confirming nanoparticle composition. Samples were analysed using carbon-coated copper grids and therefore high peaks denoting carbon and copper are also present. The other peaks present are due to medium components and elements present as part of normal bacterial composition.

Medium modification MSGM 4 (ammonium sulphate) also resulted in iron-containing nanoparticles. Although well-dispersed nanoparticles were observed (Figure S5A in Supplementary Material), it should be noted that highly agglomerated regions were also present (Figure S5B in Supplementary Material). According to Figures S5–S12 in the Supplementary Material, it could be noted that particles were highly agglomerated for medium modifications MSGM 4 to MSGM 8 and MSGM 10 to MSGM 12. Medium modification MSGM 9 (sodium nitrate and Isogro™) showed partial agglomeration; however, well dispersed iron nanoparticles were observed for most regions with a size range of 4–6 nm (Figure 4).

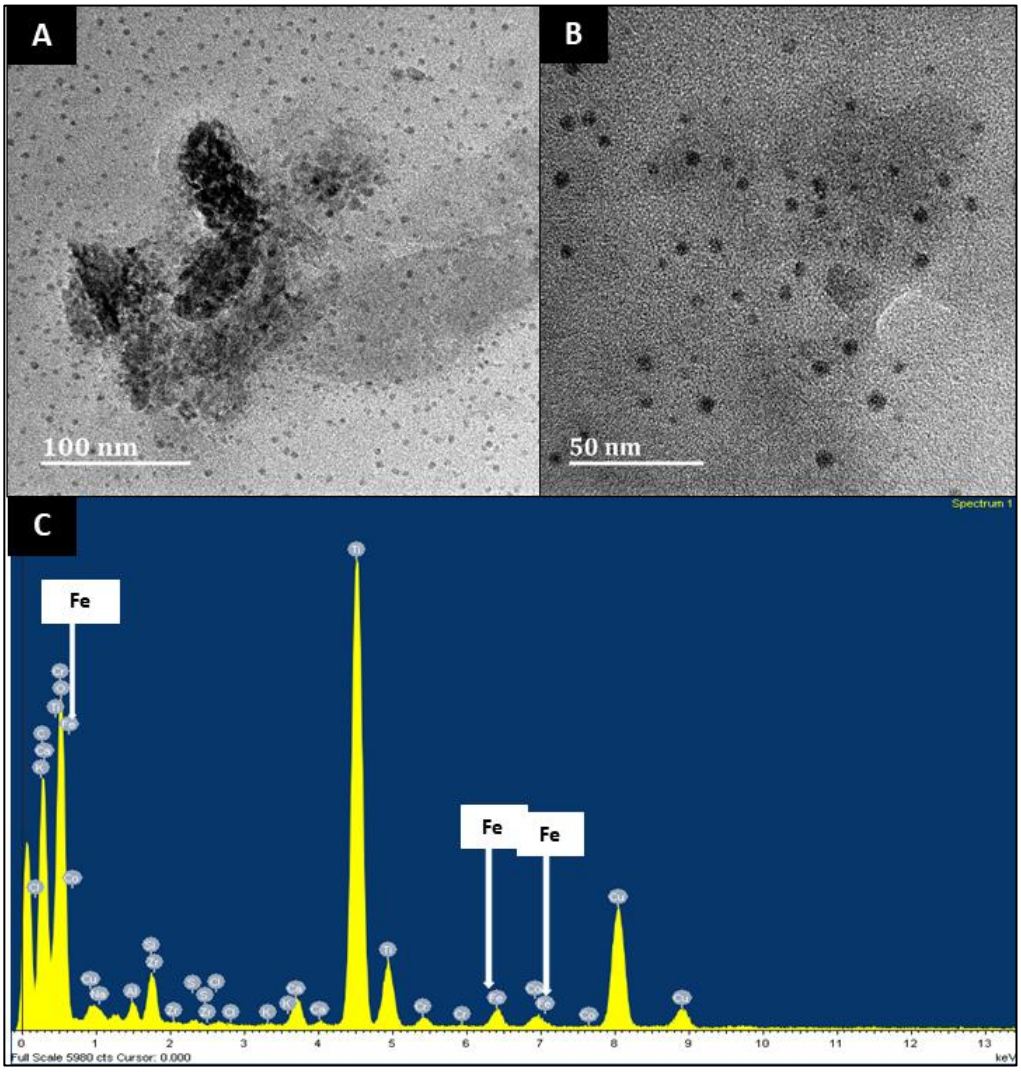


Figure 4. (**A**,**B**) TEM micrographs showing iron-containing magnetosomes formed by *M. magnetotacticum* after incubation at 30° for 48 h in MSGM 9 (sodium nitrate and Isogro™) containing iron (10 mM). Size range of nanoparticles is 4–6 nm. (**C**) EDX profile of the observed nanoparticles presented in (**A**). Distinct iron peaks are present confirming presence of iron-containing nanoparticles. Samples were analysed using carbon-coated copper grids and therefore high peaks denoting carbon and copper are also present. The other peaks present are due to medium components and elements present as part of normal bacterial composition.

MSGM original and medium modifications MSGM 6 and MSGM 9 which were supplemented with the other metals were also analysed via TEM and EDX. Figure 5 shows the TEM and EDX images obtained for silver using MSGM 9 (sodium nitrate and Isogro™), and it could be seen that the majority of the nanoparticles were rod-shaped with a width range of 2–42 nm and a length range of 32–59 nm whilst some were spherical in shape; however, these nanoparticles were also clustered. This size range is similar to the findings of Murei et al. (2021) who was also able to synthesize nanoparticles with a size range of 3–35 nm using the same MTB strain [41]. EDX confirmed the presence of silver with a high signal peak being obtained. Figures S13–S15 in the Supplementary Material show the presence of gold-containing nanoparticles when using MSGM original, MSGM 6 (sodium nitrate) and MSGM 9 (sodium nitrate and Isogro™), respectively. It could however be noted that most of the particles analysed were highly aggregated and undefined thus sizing was not possible. The high degree of agglomeration could be attributed to the magnetic potential of the nanoparticles synthesized and thus the force of attraction to each other.

According to Marcano et al. (2017), growth conditions greatly influence the final properties of the biosynthesized nanoparticles which is in agreement with the present study due to the addition of different medium components [34]. The TEM and EDX results obtained indicated the presence of iron-containing nanoparticles in MSGM original and MSGM modifications 1–12, the presence of silver in MSGM 9, and the presence of gold in MSGM original, MSGM 6 and MSGM 9, respectively.

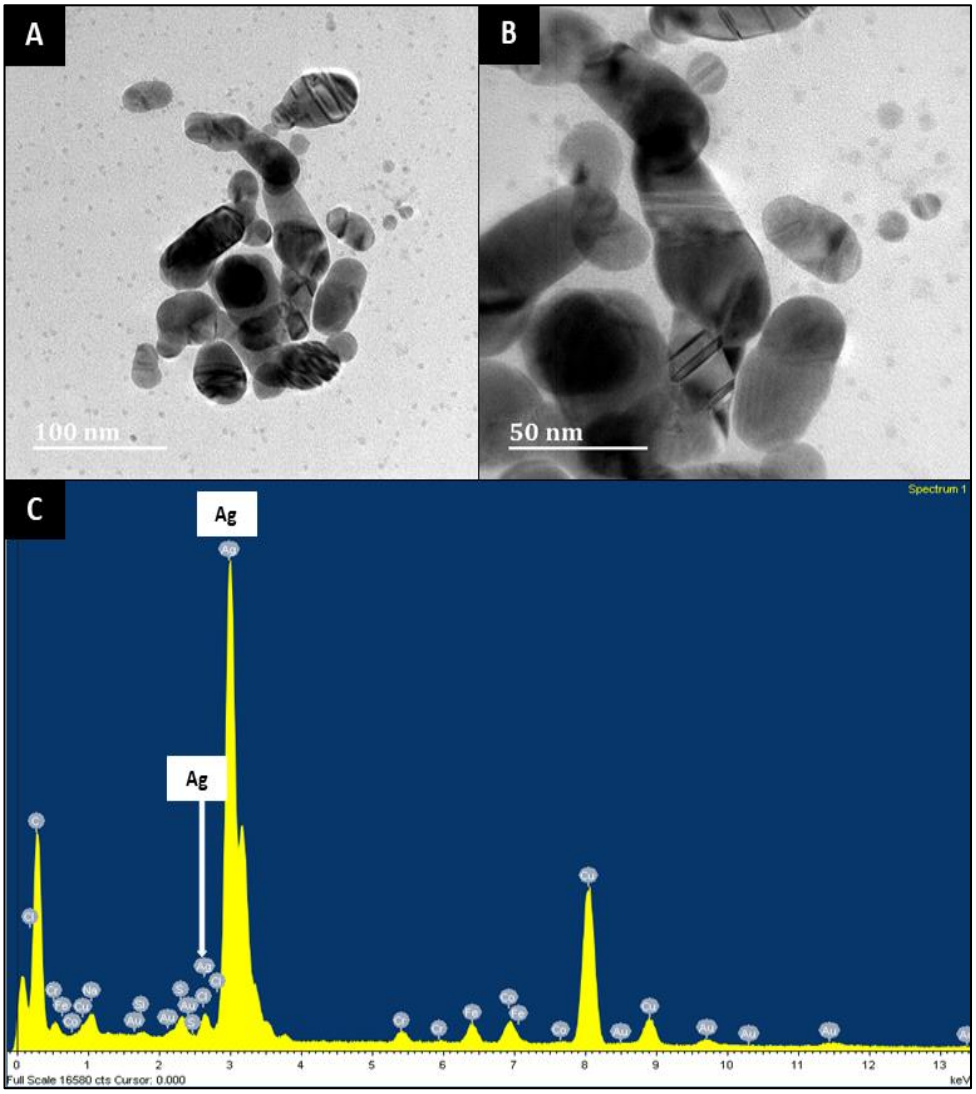


Figure 5. (**A**,**B**) TEM micrographs showing silver-containing magnetosomes formed by *M. magnetotacticum* after incubation at 30° for 48 h in MSGM 9 (sodium nitrate and Isogro™) containing silver (10 mM). Nanoparticles have a width of 2–42 nm and length of 32–59 nm. (**C**) EDX profile of the observed nanoparticles presented in (**A**). Distinct silver peaks are present confirming presence of silver-containing nanoparticles. Samples were analysed using carbon-coated copper grids and therefore high peaks denoting carbon and copper are also present. The other peaks present are due to medium components and elements present as part of normal bacterial composition.

3.2.2. DLS Analysis

Dynamic light scattering (DLS) was used to determine the hydrodynamic sizes of the metallic nanoparticles synthesized. Table 4 shows all the DLS size ranges (nm) and TEM size ranges (nm) obtained for the metallic nanoparticles that were verified using EDX analysis. It should be noted that the sizes obtained using Image J software for TEM analysis were much smaller when compared to the sizes obtained via DLS which is due to TEM

being a number-based particle size measurement whereas DLS is an intensity-based one. Therefore, DLS is very sensitive to the large particles as they were highly agglomerated and thus puts higher emphasis on the larger particle sizes whereas TEM shows stronger emphasis on the smallest components in the size distribution. This can be attributed to the difference in nature of the samples being analysed as the samples analysed via DLS were suspended in an aqueous solution which could have caused the nanoparticles to aggregate accounting for the larger sizes. The significant difference between the hydrodynamic sizes and the TEM sizes could be explained by the formation of a hydration shell on the surface of the particles present in water, which significantly affects the dynamic light scattering measurements as explained by Shipunova et al. (2018) [46]. The size range obtained for iron-containing nanoparticles using DLS was 24–68 nm for MSGM original; however, a peak with a size range of 712–6439 nm was also present and could be attributed to the high degree of agglomeration (Figure 6).

Table 4. Size and zeta potential obtained for each metal (Fe, Ag and Au) synthesized using MSGM original, MSGM 6 (sodium nitrate) and MSGM 9 (sodium nitrate and Isogro™).

MSGM Modification	Metal	Size (nm)		Zeta Potential (mV) and Stability	PDI Values
		DLS	TEM		
MSGM original	Fe	24–68 nm	6–7 nm	−26 (incipient instability)	0.534 (mid-range polydispersity)
	Ag	-	-	-	-
	Au	66–195 nm	Agglomerated	−35 (moderate stability)	0.601 (mid-range polydispersity)
MSGM 6 (sodium nitrate)	Fe	149–199 nm	Agglomerated	−40 (good stability)	0.368 (mid-range polydispersity)
	Ag	-	-	-	-
	Au	599–705 nm	Agglomerated	−23 (incipient instability)	0.574 (mid-range polydispersity)
MSGM 9 (sodium nitrate and Isogro™)	Fe	74–239 nm	4–6 nm	−44 (good stability)	0.411 (mid-range polydispersity)
	Ag	154–187 nm	2–59 nm	−40 (good stability)	0.541 (mid-range polydispersity)
	Au	270–284 nm	Agglomerated	−15 (incipient instability)	0.361 (mid-range polydispersity)

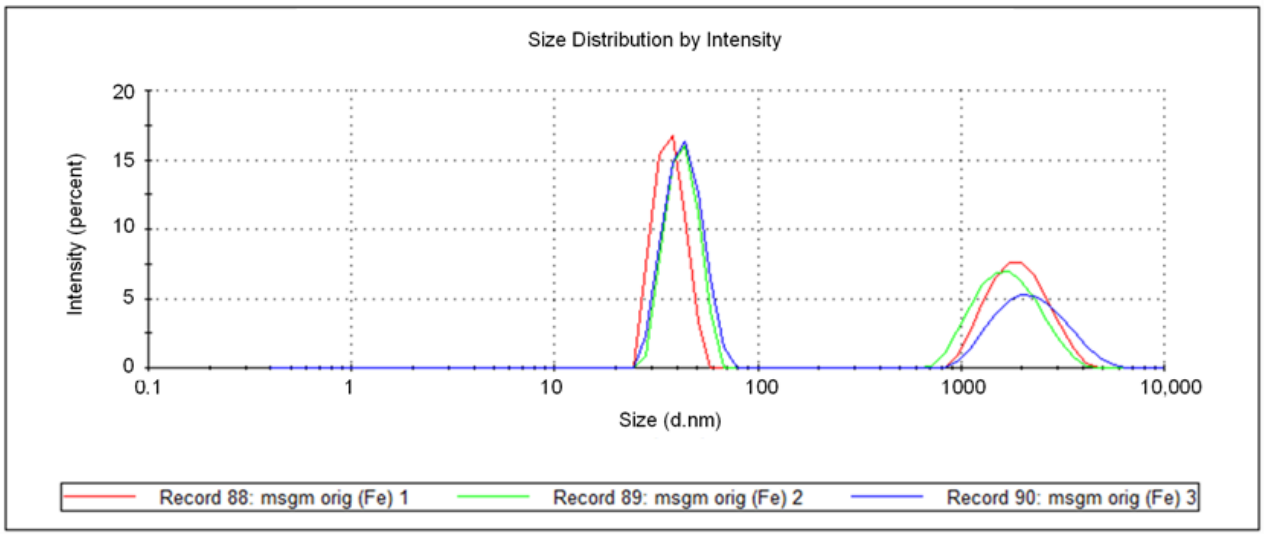


Figure 6. Size distribution intensity from DLS analysis of iron-containing magnetosomes formed by *M. magnetotacticum* after incubation at 30° for 48 h in MSGM original containing iron (10 mM).

The size range for the iron-containing nanoparticles obtained using MSGM 6 (sodium nitrate) was 149–199 nm (Figure S16 in Supplementary Material). Use of MSGM 9 (sodium nitrate and Isogro™) resulted in nanoparticles with a size range of 74–239 nm; however, there were two other peaks shown on the graph with size ranges of 255–825 nm and 4145–6439 nm, respectively, and this could also be attributed to the high degree of agglomeration (Figure 7). The size ranges obtained for gold using DLS were 66–195 nm for MSGM original (Figure S18 in Supplementary Material), 599–705 nm for MSGM 6 (sodium nitrate) (Figure S20 in Supplementary Material) and 270–284 nm for MSGM 9 (sodium nitrate and Isogro™) (Figure S21 in Supplementary Material). However, sizing using DLS could not be performed for silver using MSGM original and MSGM 6 (sodium nitrate) due to lack of verification via EDX analysis however the size range for silver obtained using MSGM 9 (sodium nitrate and Isogro™) was 12–342 nm (Figure 8).

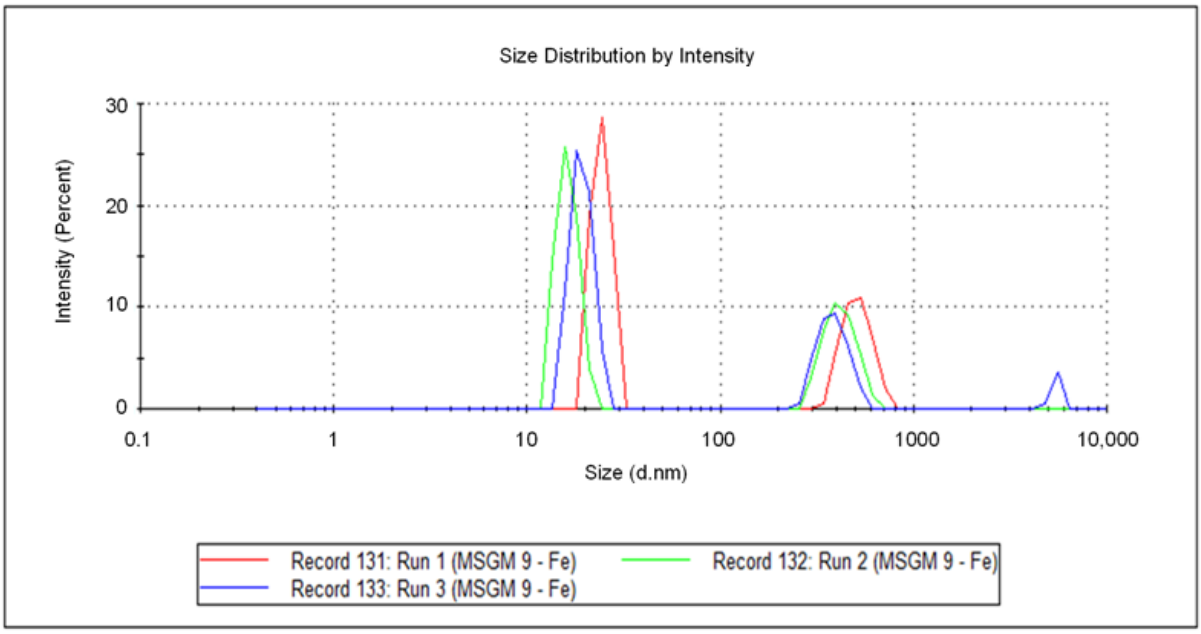


Figure 7. Size distribution intensity from DLS analysis of iron-containing magnetosomes formed by *M. magnetotacticum* after incubation at 30° for 48 h in MSGM 9 (sodium nitrate and Isogro™) containing iron (10 mM).

The zeta potential values for iron nanoparticles showed an increase in stability when using medium modifications MSGM 6 (Figure S17 in Supplementary Material) and MSGM 9 (Figure 9) with values of −40 mV and −44 mV, respectively, as compared to the value of −26 mV which was obtained for iron nanoparticles produced in MSGM original (Figure 10). This indicates that the addition of a higher concentration of sodium nitrate allowed for better stability. Silver nanoparticles were only produced using MSGM 9 (sodium nitrate and Isogro™) and showed good stability with a zeta potential value of −40 mV (Figure 11). However, gold nanoparticles showed decreasing stability with the addition of sodium nitrate and Isogro™ (Figure S22 in Supplementary Material). Gold nanoparticles produced in MSGM original, MSGM 6 (sodium nitrate) and MSGM 9 (sodium nitrate and Isogro™) had zeta potential values of −35 mV, −23 mV and −15 mV, respectively (Figures S19 and S22 in Supplementary Material), and thus sodium nitrate and Isogro™ could have a role in van der Waals forces acting upon the nanoparticles thereby facilitating their aggregation [47]. According to the graphs obtained for size and zeta potential distribution it could be noted that the nanoparticles were highly polydisperse as there was more than one peak obtained for the size distribution. The high degree of polydispersity is due to the highly agglomerated nanoparticles obtained and as seen using TEM.

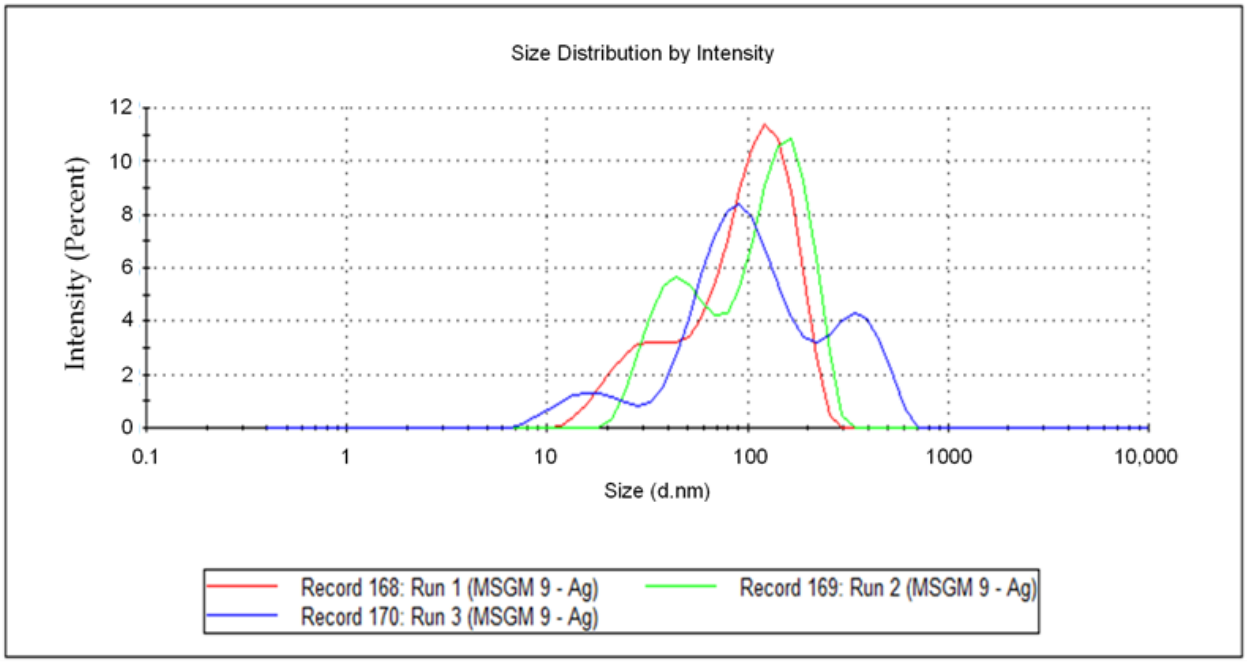


Figure 8. Size distribution intensity from DLS analysis of silver-containing magnetosomes formed by *M. magnetotacticum* after incubation at 30° for 48 h in MSGM 9 (sodium nitrate and Isogro™) containing silver (10 mM).

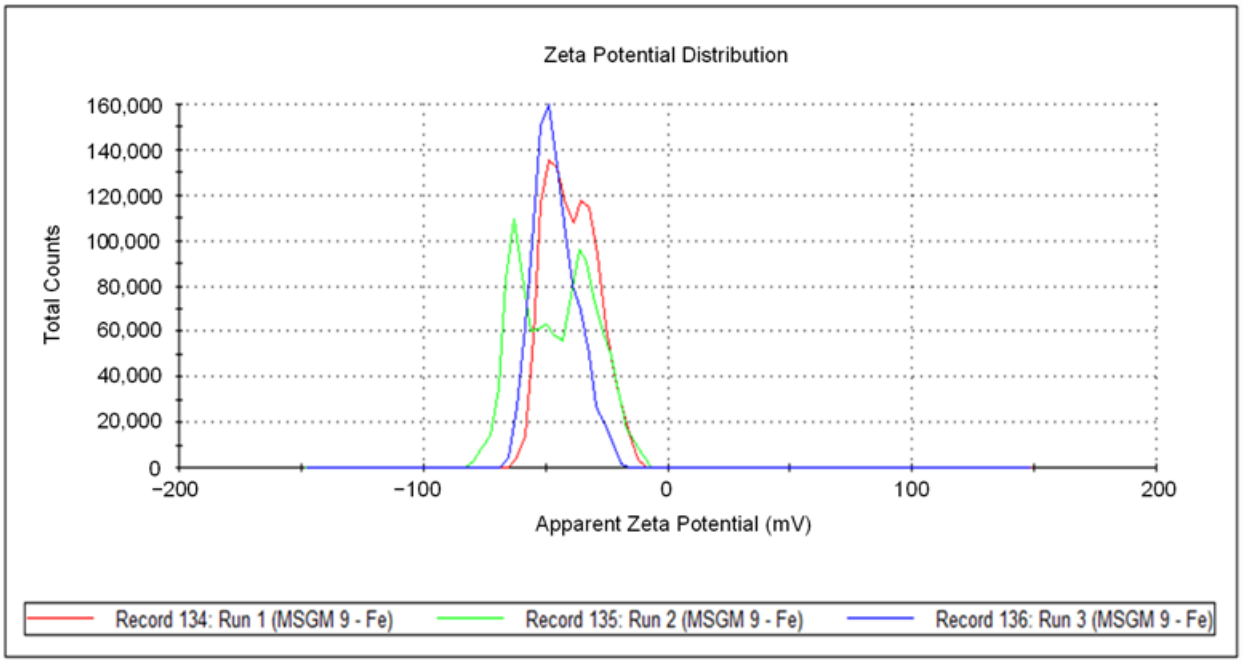


Figure 9. Zeta potential data of iron-containing magnetosomes formed by *M. magnetotacticum* after incubation at 30° for 48 h in MSGM 9 (sodium nitrate and Isogro™) containing iron (10 mM).

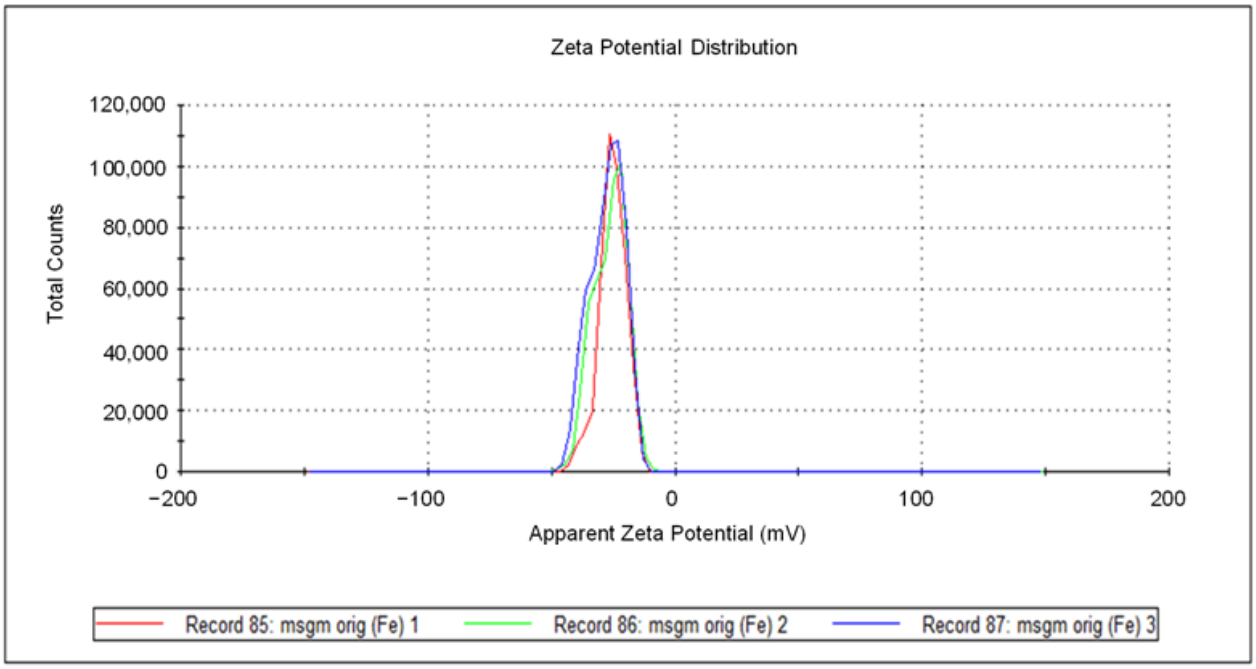


Figure 10. Zeta potential data of iron-containing magnetosomes formed by *M. magnetotacticum* after incubation at 30° for 48 h in MSGM original containing iron (10 mM).

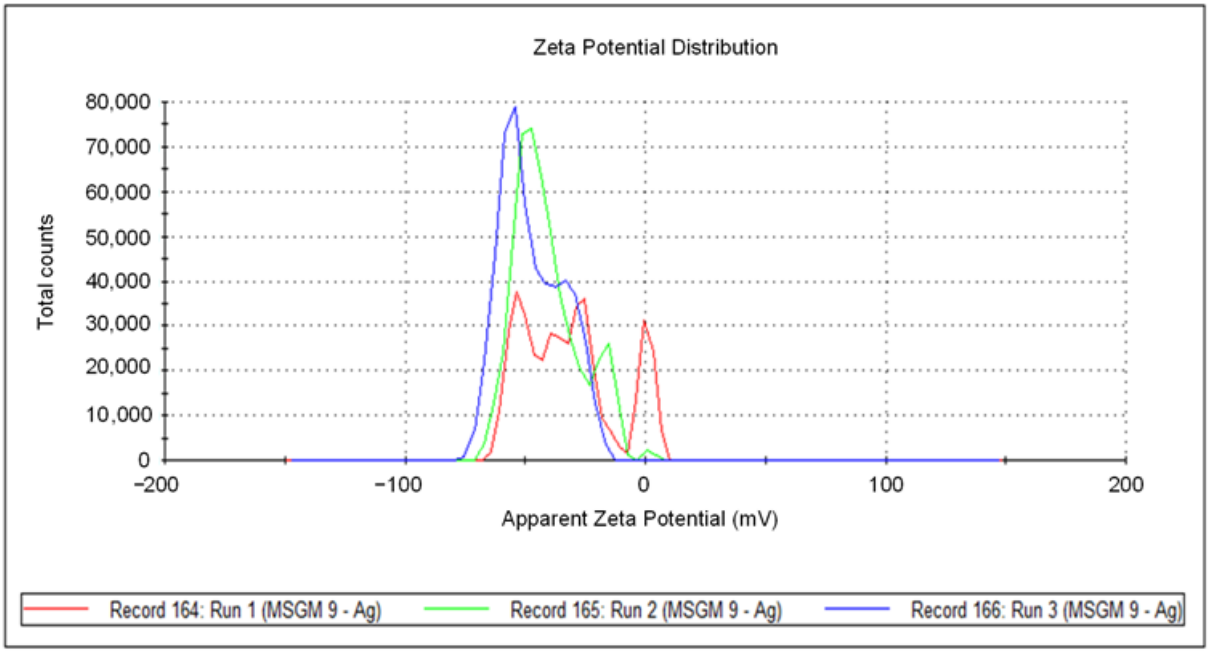


Figure 11. Zeta potential data of silver-containing magnetosomes formed by *M. magnetotacticum* after incubation at 30° for 48 h in MSGM 9 (sodium nitrate and Isogro™) containing silver (10 mM).

This study has thus demonstrated improved yield of green synthesized Fe, Ag and Au nanoparticles using the MTB strain *M. magnetotacticum*. However, further optimization to obtain non-aggregated particles especially in the case of Au needs to be investigated for downstream application. Metallic nanoparticles have a wide range of biotechnological application and a recent review by Xiong et al. (2023) clearly outlines the versatility of plasmonics in biosensors [48]. This review explains the properties and structure of photon crystals and how they can be enhanced so that they can be used to improve detection for use in a myriad of applications. Notably, AuNps coupled with quantum dots can be used

to detect actinobacteria [49], whilst poly(methyl methacrylate) opal photonic crystals were shown to detect a protein marker for prostate cancer [50]. An important factor that could also contribute to the use of magnetosomes in plasmonics is their magnetic parameters which have recently been elucidated by Ryzhov et al. (2023) [51]. Although this study presents improved yield of green synthesized metallic nanoparticles using a bacterial species, it should also be noted that the use of soluplus®, kollidon® and gelucire® as reducing and stabilizing agents for the synthesis of Au, Ag and Au-Ag hybrid nanoparticles have proven extremely successful [42–44]. In particular, it has resulted in nanoparticle platforms that have enhanced surface plasmon-coupled emission thereby making this synthetic route highly favourable for application in ultrasensitive biosensing that is even suitable for use with smartphone detection [42–44].

4. Conclusions

The present study successfully cultivated *M. magnetotacticum* in a laboratory environment using optimized media. With glucose as the sole carbon source, the bacterial growth was significantly improved and sustained compared to the other carbon sources. Using yeast extract and Isogro™ as additives also improved growth. The use of sodium nitrate (40 mM) as the sole nitrogen source improved growth at the higher concentration compared to the originally used concentration (1.4 mM) and also resulted in better growth than the sole nitrogen sources ammonium sulphate and ammonium chloride. Yeast extract significantly improved growth rates, unlike Isogro™, which achieved the highest growth in MSGM 12. The study also focused on metallic nanoparticle synthesis in a medium designed for optimal growth and maximal magnetosome nanoparticle production. The effect of the three sole carbon sources on biomass production did not significantly differ from the original MSGM carbon sources. MSGM 6, containing 40 mM of sodium nitrate, was, however, found to be the most effective in improving nanoparticle production. The highest nanoparticle yield was obtained from the exponential phase (48 h) of growth, when bacteria are most metabolically active, resulting in better metal uptake. This study found that bacterial growth and nanoparticle production did not correlate, with MSGM 1, 2, and 10 resulting in improved growth but no improvement in nanoparticle yield. It can be concluded that a fine balance between carbon and nitrogen sources is necessary for optimal magnetosome production. This study also reported the successful synthesis of nanoparticles containing iron, gold or silver by the magnetotactic bacterial strain *M. magnetotacticum*.

5. Future Scope and Perspectives

Many researchers have been actively involved in the mass cultivation of magnetosomes via the use of different MTB strains. The optimization of culture media and conditions can improve both cell growth and magnetosome yield. It is evident that there is a research gap which needs further improvement to simultaneously improve both nanoparticle production and bacterial growth whilst also improving the overall expenses involved in the preparation of culture medium and optimization of physiological conditions. A possible way to improve the use of the nanoparticles synthesized in the present study could be by evaluating the use of capping agents in future studies to stabilize the nanoparticles thus preventing the nanoparticles from agglomerating. In addition, there are various areas of this field that can be explored, one such being genetically engineering specific magnetosome proteins for improved functionalization of the magnetosomal membrane and for improved purification of magnetosomes which are important issues that are currently limiting their practical applicability, specifically in biomedicine and biotechnology where purified magnetosomes are needed.

Supplementary Materials: The following supporting information can be downloaded at: https://www.mdpi.com/article/10.3390/app13148491/s1, Table S1: ATCC medium 1653-Revised Magnetic *Spirillum* Growth Medium (MSGM) composition, Table S2: Composition of Wolfe's Vitamin & Mineral solutions, Table S3: MSGM media modifications for bacterial growth curves in methodology, Table S4: Statistical analysis using Pearson's correlation coefficient (r) for each MSGM modification vs MSGM

original supplemented with iron, Table S5: Statistical analysis results showing p-values obtained using one way analysis of variance (ANOVA) for determination of statistical significant difference between nanoparticle dry weight yields for all MSGM modifications supplemented with iron, Table S6: Statistical analysis results showing p-values obtained using ANOVA for determination of statistical significant difference between nanoparticle dry weight yields between the three different phases of isolation using MSGM 6 (sodium nitrate), Figure S1: Growth curves of *M. magnetotacticum* in MSGM original and media modifications MSGM 1, 2, 8, 10, 11 and 12 at 30 °C with iron as the metal source, Figure S2: (A,B) TEM micrographs showing iron containing magnetosomes formed by *M. magnetotacticum* after incubation at 30° for 48 h in MSGM 1 (glucose) containing iron (10 mM). (C) EDX profile of the observed nanoparticles in (A), Figure S3: (A,B) TEM micrographs showing iron containing magnetosomes formed by *M. magnetotacticum* after incubation at 30° for 48 hours in MSGM 2 (sodium pyruvate) containing iron (10 mM). Size range of nanoparticles is 13–81 nm. (C) EDX profile of the observed nanoparticles in (A), Figure S4: (A,B) TEM micrographs showing iron containing magnetosomes formed by *M. magnetotacticum* after incubation at 30° for 48 h in MSGM 3 (lactic acid) containing iron (10 mM). (C) EDX profile of the observed nanoparticles in (A), Figure S5: (A,B) TEM micrographs showing iron containing magnetosomes formed by *M. magnetotacticum* after incubation at 30° for 48 h in MSGM 4 (ammonium sulphate) containing iron (10 mM). (C) EDX profile of the observed nanoparticles in (A), Figure S6: (A,B) TEM micrographs showing iron containing magnetosomes formed by *M. magnetotacticum* after incubation at 30° for 48 h in MSGM 5 (ammonium chloride) containing iron (10 mM). (C) EDX profile of the observed nanoparticles in (A), Figure S7: (A,B) TEM micrographs showing iron containing magnetosomes formed by *M. magnetotacticum* after incubation at 30° for 48 h in MSGM 6 (sodium nitrate) containing iron (10 mM). (C) EDX profile of the observed nanoparticles in (A), Figure S8: (A,B) TEM micrographs showing iron containing magnetosomes formed by *M. magnetotacticum* after incubation at 30° for 48 h in MSGM 7 (ammonium sulphate and sodium nitrate) containing iron (10 mM). (C) EDX profile of the observed nanoparticles in (A), Figure S9: (A,B) TEM micrographs showing iron containing magnetosomes formed by *M. magnetotacticum* after incubation at 30° for 48 h in MSGM 8 (ammonium sulphate, sodium nitrate and yeast extract) containing iron (10 mM). (C) EDX profile of the observed nanoparticles in (A), Figure S10: (A,B) TEM micrographs showing iron containing magnetosomes formed by *M. magnetotacticum* after incubation at 30° for 48 h in MSGM 10 (glucose and sodium nitrate) containing iron (10 mM). (C) EDX profile of the observed nanoparticles in (A), Figure S11: (A,B) TEM micrographs showing iron containing magnetosomes formed by *M. magnetotacticum* after incubation at 30° for 48 h in MSGM 11 (glucose, sodium nitrate and ammonium sulphate) containing iron (10 mM). (C) EDX profile of the observed nanoparticles in (A), Figure S12: (A,B) TEM micrographs showing iron containing magnetosomes formed by *M. magnetotacticum* after incubation at 30° for 48 h in MSGM 12 (glucose, sodium nitrate, ammonium sulphate and yeast extract) containing iron (10 mM). (C) EDX profile of the observed nanoparticles in (A), Figure S13: (A,B) TEM micrographs showing gold containing magnetosomes formed by *M. magnetotacticum* after incubation at 30° for 48 h in MSGM original containing gold (10 mM). (C) EDX profile of the observed nanoparticles in (A), Figure S14: (A,B) TEM micrographs showing gold containing magnetosomes formed by *M. magnetotacticum* after incubation at 30° for 48 h in MSGM 6 (sodium nitrate) containing gold (10 mM). (C) EDX profile of the observed nanoparticles in (A), Figure S15: (A,B) TEM micrographs showing gold containing magnetosomes formed by *M. magnetotacticum* after incubation at 30° for 48 h in MSGM 9 (sodium nitrate and Isogro™) containing gold (10 mM). (C) EDX profile of the observed nanoparticles in (A), Figure S16: Size distribution intensity from DLS analysis of iron containing magnetosomes formed by *M. magnetotacticum* after incubation at 30° for 48 h in MSGM 6 (sodium nitrate) containing iron (10 mM), Figure S17: Zeta potential data of iron containing magnetosomes formed by *M. magnetotacticum* after incubation at 30° for 48 h in MSGM 6 (sodium nitrate) containing iron (10 mM), Figure S18: Size distribution intensity from DLS analysis of gold containing magnetosomes formed by *M. magnetotacticum* after incubation at 30° for 48 h in MSGM original containing gold (10 mM), Figure S19: Zeta potential data of gold containing magnetosomes formed by *M. magnetotacticum* after incubation at 30° for 48 h in MSGM original containing gold (10 mM), Figure S20: Size distribution intensity from DLS analysis of gold containing magnetosomes formed by *M. magnetotacticum* after incubation at 30° for 48 hours in MSGM 6 (sodium nitrate) containing gold (10 mM), Figure S21: Size distribution intensity from DLS analysis of gold containing magnetosomes formed by *M. magnetotacticum* after incubation at 30° for 48 h in MSGM 9 (sodium nitrate and Isogro™) containing gold (10 mM), and Figure S22: Zeta potential data of gold containing

magnetosomes formed by *M. magnetotacticum* after incubation at 30° for 48 h in MSGM 9 (sodium nitrate and Isogro™) containing gold (10 mM).

Author Contributions: Conceptualization, R.E.S. and K.P.; methodology, R.E.S. and K.P.; formal analysis, R.E.S. and K.P.; investigation, R.E.S.; resources, K.P.; writing—original draft preparation, R.E.S., K.P. and A.G.; writing—review and editing, R.E.S., K.P. and A.G.; supervision, K.P.; project administration, K.P.; funding acquisition, K.P. All authors have read and agreed to the published version of the manuscript.

Funding: The student was funded by The National Research Foundation (NRF), grant number 131885. This work was funded by the National Research Foundation of South Africa (Grant Number: SRUG2203291132). The funding body however had no role in study design; in the collection, analysis and interpretation of data; in the writing of the report; and in the decision to submit the article for publication.

Institutional Review Board Statement: Not applicable.

Informed Consent Statement: Not applicable.

Data Availability Statement: The data presented in this study are available in this article and in the associated Supplementary Material.

Acknowledgments: Sincere thanks to NRF for financial assistance without which this study would have not been possible and to Philip Christopher and Subashen Naidu from the Microscopy and Microanalysis unit (MMU) (UZN, Westville) for their assistance in transmission electron microscopy and EDX analysis.

Conflicts of Interest: The authors declare no conflict of interest. The funders had no role in the design of the study; in the collection, analyses or interpretation of data; in the writing of the manuscript; or in the decision to publish the results.

References

1. Faramarzi, M.A.; Sadighi, A. Insights into biogenic and chemical production of inorganic nanomaterials and nanostructures. *Adv. Colloid Interface Sci.* **2013**, *189*, 1–20. [CrossRef]
2. Lefèvre, C.T.; Bazylinski, D.A. Ecology, diversity, and evolution of magnetotactic bacteria. *Microbiol. Mol. Biol. Rev.* **2013**, *77*, 497–526. [CrossRef]
3. Araujo, A.C.V.; Abreu, F.; Silva, K.T.; Bazylinski, D.A.; Lins, U. Magnetotactic bacteria as potential sources of bioproducts. *Mar. Drugs* **2015**, *13*, 389–430. [CrossRef]
4. Bazylinski, D.A.; Frankel, R.B.; Heywood, B.R.; Mann, S.; King, J.W.; Donaghay, P.L.; Hanson, A.K.J.A. Controlled Biomineralization of Magnetite (Fe (inf3) O (inf4)) and Greigite (Fe (inf3) S (inf4)) in a Magnetotactic Bacterium. *Appl. Environ. Microbiol.* **1995**, *61*, 3232–3239. [CrossRef]
5. Lins, U.; Keim, C.N.; Evans, F.F.; Farina, M.; Buseck, P.R. Magnetite (Fe_3O_4) and greigite (Fe_3S_4) crystals in multicellular magnetotactic prokaryotes. *Geomicrobiol. J.* **2007**, *24*, 43–50. [CrossRef]
6. Heyen, U.; Schüler, D. Growth and magnetosome formation by microaerophilic Magnetospirillum strains in an oxygen-controlled fermentor. *Appl. Microbiol. Biotechnol.* **2003**, *61*, 536–544. [CrossRef]
7. Bazylinski, D.A.; Frankel, R.B. Magnetosome formation in prokaryotes. *Nat. Rev. Microbiol.* **2004**, *2*, 217–230. [CrossRef]
8. Vargas, G.; Cypriano, J.; Correa, T.; Leão, P.; Bazylinski, D.A.; Abreu, F. Applications of magnetotactic bacteria, magnetosomes and magnetosome crystals in biotechnology and nanotechnology: Mini-review. *Molecules* **2018**, *23*, 2438. [CrossRef]
9. Składanowski, M.; Wypij, M.; Laskowski, D.; Golińska, P.; Dahm, H.; Rai, M. Silver and gold nanoparticles synthesized from Streptomyces sp. isolated from acid forest soil with special reference to its antibacterial activity against pathogens. *J. Clust. Sci.* **2017**, *28*, 59–79. [CrossRef]
10. Ali, I.; Peng, C.; Khan, Z.M.; Naz, I. Yield cultivation of magnetotactic bacteria and magnetosomes: A review. *J. Basic Microbiol.* **2017**, *57*, 643–652. [CrossRef]
11. Shanmugam, N.; Rajkamal, P.; Cholan, S.; Kannadasan, N.; Sathishkumar, K.; Viruthagiri, G.; Sundaramanickam, A. Biosynthesis of silver nanoparticles from the marine seaweed Sargassum wightii and their antibacterial activity against some human pathogens. *Appl. Nanosci.* **2014**, *4*, 881–888. [CrossRef]
12. Rajasulochana, P.; Dhamotharan, R.; Murugakoothan, P.; Murugesan, S.; Krishnamoorthy, P. Biosynthesis and characterization of gold nanoparticles using the alga Kappaphycus alvarezii. *Int. J. Nanosci.* **2010**, *9*, 511–516. [CrossRef]
13. Mata, Y.; Torres, E.; Blazquez, M.; Ballester, A.; González, F.; Munoz, J. Gold (III) biosorption and bioreduction with the brown alga Fucus vesiculosus. *J. Hazard. Mater.* **2009**, *166*, 612–618. [CrossRef]
14. Senapati, S.; Syed, A.; Moeez, S.; Kumar, A.; Ahmad, A. Intracellular synthesis of gold nanoparticles using alga Tetraselmis kochinensis. *Mater. Lett.* **2012**, *79*, 116–118. [CrossRef]

15. Fernández-Castané, A.; Li, H.; Thomas, O.R.; Overton, T.W. Development of a simple intensified fermentation strategy for growth of Magnetospirillum gryphiswaldense MSR-1: Physiological responses to changing environmental conditions. *New Biotechnol.* **2018**, *46*, 22–30. [CrossRef]
16. Jajan, L.H.G.; Hosseini, S.N.; Ghorbani, M.; Mousavi, S.F.; Ghareyazie, B.; Abolhassani, M. Effects of environmental conditions on high-yield magnetosome production by Magnetospirillum gryphiswaldense MSR-1. *Iran. Biomed. J.* **2019**, *23*, 209–219.
17. Berny, C.; Le Fèvre, R.; Guyot, F.; Blondeau, K.; Guizonne, C.; Rousseau, E.; Bayan, N.; Alphandéry, E. A method for producing highly pure magnetosomes in large quantity for medical applications using Magnetospirillum gryphiswaldense MSR-1 magnetotactic bacteria amplified in minimal growth media. *Front. Bioeng. Biotechnol.* **2020**, *8*, 1–13. [CrossRef]
18. Blakemore, R. Magnetotactic bacteria. *Science* **1975**, *190*, 377–379. [CrossRef]
19. Zhang, S.; Yan, L.; Li, H.; Liu, H. Optimal conditions for growth and magnetosome formation of Acidithiobacillus ferrooxidans. *Afr. J. Microbiol. Res.* **2012**, *6*, 6142–6151. [CrossRef]
20. Hadadian, Y.; Sampaio, D.R.; Ramos, A.P.; Carneiro, A.A.; Mozaffari, M.; Cabrelli, L.C.; Pavan, T.Z. Synthesis and characterization of zinc substituted magnetite nanoparticles and their application to magneto-motive ultrasound imaging. *J. Magn. Magn. Mater.* **2018**, *465*, 33–43. [CrossRef]
21. Moodley, J.S.; Krishna, S.N.; Pillay, K.; Govender, P. Production, characterization and antimicrobial activity of silver nanoparticles produced by Pediococcus acidilactici. *Dig. J. Nanomater. Biostruct.* **2018**, *13*, 77–86.
22. Moodley, J.S.; Krishna, S.B.N.; Pillay, K.; Sershen, F.; Govender, P. B.N.; Pillay, K.; Govender, P. Green synthesis of silver nanoparticles from Moringa oleifera leaf extracts and its antimicrobial potential. *Adv. Nat. Sci. Nanosci. Nanotechnol.* **2018**, *9*, 015011.
23. Schneider, C.A.; Rasband, W.S.; Eliceiri, K.W. NIH Image to ImageJ: 25 years of image analysis. *Nat. Method* **2012**, *9*, 671–675. [CrossRef]
24. Schober, P.; Boer, C.; Schwarte, L.A. Correlation Coefficients: Appropriate Use and Interpretation. *Anesth. Analg.* **2018**, *126*, 1763–1768. [CrossRef]
25. Bren, A.; Park, J.O.; Towbin, B.D.; Dekel, E.; Rabinowitz, J.D.; Alon, U. Glucose becomes one of the worst carbon sources for E. coli on poor nitrogen sources due to suboptimal levels of cAMP. *Sci. Rep.* **2016**, *6*, 24834. [CrossRef]
26. Hantzidiamantis, P.J.; Lappin, S.L. *Physiology, Glucose*; StatPearls Publishing: Tampa, FL, USA, 2019.
27. Liu, Y.; Li, G.R.; Guo, F.F.; Jiang, W.; Li, Y.; Li, L.J. Large-scale production of magnetosomes by chemostat culture of Magnetospirillum gryphiswaldense at high cell density. *Microb. Cell Factories* **2010**, *9*, 99. [CrossRef]
28. Bazylinski, D.A.; Blakemore, R.J. Denitrification and assimilatory nitrate reduction in Aquaspirillum magnetotacticum. *Appl. Environ. Microbiol.* **1983**, *46*, 1118–1124. [CrossRef]
29. Yamazaki, T.; Oyanagi, H.; Fujiwara, T.; Fukumori, Y. Nitrite reductase from the magnetotactic bacterium Magnetospirillum magnetotacticum: A novel cytochrome cd1 with Fe (II): Nitrite oxidoreductase activity. *Eur. J. Biochem.* **1995**, *233*, 665–671. [CrossRef]
30. Taoka, A.; Yoshimatsu, K.; Kanemori, M.; Fukumori, Y. Nitrate reductase from the magnetotactic bacterium Magnetospirillum magnetotacticum MS-1: Purification and sequence analyses. *Can. J. Microbiol.* **2003**, *49*, 197–206. [CrossRef]
31. Ardelean, I.I.; Moisescu, C.; Popoviciu, D.R. Magnetotactic bacteria and their potential for terraformation. In *From Fossils to Astrobiology: Records of Life on Earth and Search for Extraterrestrial Biosignatures*; Springer: Dordrecht, The Netherlands, 2008; pp. 335–350.
32. Muller, F.D.; Schuler, D.; Pfeiffer, D. A Compass To Boost Navigation: Cell Biology of Bacterial Magnetotaxis. *J. Bacteriol.* **2020**, *202*, e00398-20. [CrossRef]
33. Rolfe, M.D.; Rice, C.J.; Lucchini, S.; Pin, C.; Thompson, A.; Cameron, A.D.; Alston, M.; Stringer, M.F.; Betts, R.P.; Baranyi, J. Lag phase is a distinct growth phase that prepares bacteria for exponential growth and involves transient metal accumulation. *J. Bacteriol.* **2012**, *194*, 686–701. [CrossRef] [PubMed]
34. Marcano, L.; García-Prieto, A.; Muñoz, D.; Barquín, L.F.; Orue, I.; Alonso, J.; Muela, A.; Fdez-Gubieda, M.J. Influence of the bacterial growth phase on the magnetic properties of magnetosomes synthesized by Magnetospirillum gryphiswaldense. *Biochim. Biophys. Acta BBA Gen. Subj.* **2017**, *1861*, 1507–1514. [CrossRef]
35. Sun, J.-B.; Zhao, F.; Tang, T.; Jiang, W.; Tian, J.-s.; Li, Y.; Li, J.-L. High-yield growth and magnetosome formation by Magnetospirillum gryphiswaldense MSR-1 in an oxygen-controlled fermentor supplied solely with air. *Appl. Microbiol. Biotechnol.* **2008**, *79*, 389–397. [CrossRef] [PubMed]
36. Liu, J.; Ding, Y.; Jiang, W.; Tian, J.; Li, Y.; Li, J. A mutation upstream of an ATPase gene significantly increases magnetosome production in Magnetospirillum gryphiswaldense. *Chin. Sci. Bull.* **2008**, *81*, 551–558. [CrossRef]
37. Khan, I.; Saeed, K.; Khan, I. Nanoparticles: Properties, applications and toxicities. *Arab. J. Chem.* **2019**, *12*, 908–931. [CrossRef]
38. Gorup, L.F.; Neto, F.N.S.; Kubo, A.M.; Souza, J.A.S.; Fernandes, R.A.; Fernandes, G.L.; Monteiro, D.R.; Barbosa, D.B.; Camargo, E.R. Nanostructured functional materials: Silver nanoparticles in polymer for the generation of antimicrobial characteristics. In *Recent Advances in Complex Functional Materials*; Springer: Berlin/Heidelberg, Germany, 2017; pp. 271–292.
39. McNamara, K.; Tofail, S.A. Nanoparticles in biomedical applications. *Adv. Phys. X* **2017**, *2*, 54–88. [CrossRef]
40. Wang, L.; Hu, C.; Shao, L. The antimicrobial activity of nanoparticles: Present situation and prospects for the future. *Int. J. Nanomed.* **2017**, *12*, 1227–1249. [CrossRef]

41. Murei, A.; Pillay, K.; Govender, P.; Thovhogi, N.; Gitari, W.M.; Samie, A. Synthesis, Characterization and In Vitro Antibacterial Evaluation of Pyrenacantha grandiflora Conjugated Silver Nanoparticles. *Nanomaterials* **2021**, *11*, 1568. [CrossRef]
42. Rai, A.; Bhaskar, S.; Ramamurthy, S.S. Plasmon-Coupled Directional Emission from Soluplus-Mediated AgAu Nanoparticles for Attomolar Sensing Using a Smartphone. *ACS Appl. Nano Mater.* **2021**, *4*, 5940–5953. [CrossRef]
43. Rai, A.; Bhaskar, S.; Ganesh, K.M.; Ramamurthy, S.S. Cellphone-based attomolar tyrosine sensing based on Kollidon-mediated bimetallic nanorod in plasmon-coupled directional and polarized emission architecture. *Mater. Chem. Phys.* **2022**, *285*, 126129. [CrossRef]
44. Rai, A.; Bhaskar, S.; Ganesh, K.M.; Ramamurthy, S.S. Gelucire®-mediated heterometallic AgAu nanohybrid engineering for femtomolar cysteine detection using smartphone-based plasmonics technology. *Mater. Chem. Phys.* **2022**, *279*, 125747–125775. [CrossRef]
45. Kresnowati, M.T.A.P.; Wijaya, A.W.; Andry, A. Nanomagnetic Particle Production: Effect of Carbon and Iron Sources. *J. Eng. Technol. Sci.* **2016**, *48*, 645–654. [CrossRef]
46. Shipunova, V.O.; Kotelnikova, P.A.; Aghayeva, U.F.; Stremovskiy, O.A.; Schulga, A.A.; Nikitin, M.P.; Deyev, S.M. Data on characterization of magnetic nanoparticles stabilized with fusion protein of Barstar and C-term part of Mms6. *Data Brief* **2018**, *21*, 1659–1663. [CrossRef] [PubMed]
47. Joseph, E.; Singhvi, G. Multifunctional nanocrystals for cancer therapy: A potential nanocarrier. *Nanomater. Drug Deliv. Ther.* **2019**, 91–116. [CrossRef]
48. Xiong, Y.; Shepherd, S.; Tibbs, J.; Bacon, A.; Liu, W.; Akin, L.D.; Ayupova, T.; Bhaskar, S.; Cunningham, B.T. Photonic Crystal Enhanced Fluorescence: A Review on Design Strategies and Applications. *Micromachines* **2023**, *14*, 668. [CrossRef]
49. Zhang, H.; Lv, J.; Jia, Z. Efficient Fluorescence Resonance Energy Transfer between Quantum Dots and Gold Nanoparticles Based on Porous Silicon Photonic Crystal for DNA Detection. *Sensors* **2017**, *17*, 1078. [CrossRef]
50. Hu, S.; Xu, H.; Zhou, B.; Xu, S.; Shen, B.; Dong, B.; Yin, Z.; Xu, S.; Sun, L.; Lv, J.; et al. Double Stopband Bilayer Photonic Crystal Based Upconversion Fluorescence PSA Sensor. *Sens. Actuators B Chem.* **2021**, *326*, 128816–128826. [CrossRef]
51. Ryzhov, V.; Deriglazov, V.; Grouzdev, D.; Koziaeva, V.; Kiselev, I.; Larionov, I.; Gareev, K.; Sitkov, N.; Zimina, T.; Marchenko, Y.; et al. Biogenic Nanomagnetic Carriers Derived from Magnetotactic Bacteria: Magnetic Parameters of Magnetosomes Inside *Magnetospirillum* spp. *Appl. Sci.* **2023**, *13*, 2431. [CrossRef]

Disclaimer/Publisher's Note: The statements, opinions and data contained in all publications are solely those of the individual author(s) and contributor(s) and not of MDPI and/or the editor(s). MDPI and/or the editor(s) disclaim responsibility for any injury to people or property resulting from any ideas, methods, instructions or products referred to in the content.